[i.e., superoxide radical ($^{\bullet}O_2^-$) and nitric oxide (NO), respectively] [3–6]. Peroxynitrite ($ONOO^-$), the reaction product of $^{\bullet}O_2^-$ and NO, is a highly reactive oxidant and has recently been demonstrated to act as a major mediator in the neurotoxicity induced by Aβ-activated microglia in vitro [7]. Indeed, the levels of nitrotyrosine, which is a product of the reaction of $ONOO^-$ with tyrosine residues and considered as a permanent footprint of $ONOO^-$, have been reported to increase in AD brains [8]. Taken together, the inhibition of Aβ-induced microglial production of inflammatory cytokines including TNF-α and free radicals such as NO, $^{\bullet}O_2^-$, and subsequent formation of $ONOO^-$ appears to be neuroprotective and a potentially useful treatment for AD.

Phospholipids such as phosphatidylserine (PS) and phosphatidylcholine (PC) have been shown to modulate the immune functions of phagocytes. PC, a major component of the outer leaflet of plasma membrane, has been demonstrated to reduce the production of ROS in lipopolysaccharide (LPS)/phorbol 12-myristate-13-acetate (PMA)-activated monocytes [9]. On the other hand, abnormal exposure of PS, which is normally sequestered in the inner leaflet of plasma membrane, in the early phase of apoptosis is an essential determinant for the recognition and ingestion of apoptotic cells by phagocytes [10]. After the engulfment of apoptotic cells, macrophages are well known to actively suppress the inflammatory response through the release of anti-inflammatory mediators, thereby decreasing the secretion of various proinflammatory cytokines [11]. Furthermore, PS-containing liposomes have been shown to mimic the effects of apoptotic cells on macrophages [12] and on microglia [13,14] through surface molecules that recognize PS. Intriguingly, PS has also been reported to be one of the nootropics that can be used as nonprescription memory or cognitive enhancers [15]. According to in vivo studies, PS treatment has been demonstrated to ameliorate the impaired functions of learning and memory on a variety of tasks in aged rats [16] and PS-containing liposomes have been shown to protect LPS-induced impairment of long-term potentiation (LTP) in adult rats [17]. In human clinical trials, some studies have shown that the oral administration of bovine brain cortex-derived PS improves the behavior and cognitive performances of patients with senile dementia [18,19].

For the above-noted reasons, we evaluated the effects of liposomes comprising PS and PC on the Aβ and interferon-γ (IFN-γ)-induced microglial production of proinflammatory molecules such as TNF-α, NO, and $^{\bullet}O_2^-$. Especially, $^{\bullet}O_2^-$ is a key molecule in the oxidative stress involved in the pathogenesis of AD because $^{\bullet}O_2^-$ is not only a tally of NO for $ONOO^-$ formation but also a limiting factor for $ONOO^-$ formation [20,21]. Furthermore, $^{\bullet}O_2^-$ is a precursor of other types of ROS such as hydrogen peroxide (H_2O_2) and hydroxyl radical ($^{\bullet}OH$), and ROS has also been reported to mediate proinflammatory signaling in activated microglia, thereby amplifying the TNF-α production [22]. We, therefore, measured the microglial $^{\bullet}O_2^-$ production specifically and directly using electron spin resonance (ESR) with the spin-trap technique. To our knowledge, this is the first report to directly trap $^{\bullet}O_2^-$ associated with Aβ-stimulated microglia.

Materials and methods

Aβ peptides

The Aβ25–35 peptides used in this study were purchased from AnaSpec (San Jose, CA). Purity was certified by high-performance liquid chromatography–mass spectrometry for each of the peptide. The peptides were resuspended in sterile double-deionized water, aliquoted at 5 mg/ml, and kept at −20°C. We preliminarily confirmed that neither PS/PC liposomes (data not shown) nor IFN-γ [4] affected the amyloid fibril structure of the Aβ25–35 peptides using a thioflavine-T fluorometric assay.

Chemicals and reagents

A spin-trap 5-(diethoxyphosphoryl)-5-methyl-1-pyroline-*N*-oxide (DEPMPO), LPS, and diethylenetriamine pentaacetic acid (DTPA) were purchased from Sigma Chemicals (St. Louis, MO). Superoxide dismutase (SOD; from bovine erythrocytes, 3500 U/mg), catalase (from beef liver, 11500 U/mg), xanthine, and xanthine oxidase were purchased from Wako (Osaka, Japan). The final concentrations of SOD and catalase correspond to the enzyme activities per volume as described in a previous report [23]. Recombinant IFN-γ was purchased from Genzyme (Cambridge, MA). Recombinant mouse granulocyte macrophage colony stimulating factor (GM-CSF) was purchased from R&D systems (Minneapolis, MN). Porcine brain-derived-L-α-PS, egg-derived-L-α-PC, 4-nitrobenz-2-oxa-1,3-diazole (NBD)-labeled PS, and NBD-labeled PC were purchased from Avanti Polar Lipids (Alabaster, AL).

Preparation of liposomes

The liposomes were prepared as previously described [24]. In brief, a mixture of 12 mM PS and 33 mM PC in chloroform was placed in a test tube. The liposomes were composed of either a combination of PS and PC at a molar ratio of 3:7 (PS:PC) (PS/PC liposomes) or PC only (PC liposomes). The solvent was removed in a rotary evaporator at 30°C under reduced pressure and then dried by a desiccator for 1 h. The desiccated lipids were dispersed with a vortex mixer in phosphate-buffered saline (PBS) (pH 7.4) to obtain a final concentration of 10 mM total lipids. The lipid suspensions were subsequently sonicated (Tomy UR-20P, Tokyo, Japan) for 10 min on ice. The liposome solutions were centrifuged and then the supernatants were used for the assays. Using either NBD-labeled PS or NBD-labeled PC, NBD-labeled PS/PC liposomes and NBD-labeled PC liposomes were prepared by the same methods as described above.

Microglial cell cultures

Primary microglial cells were isolated from mixed cell cultures from the cerebral cortex of 3-day-old Wister rats according to the methods described previously [4,25]. The cerebral cortex was minced and treated with papain (90 U/ml) and DNase (2000 U/ml) at 37°C for 15 min. The mechanically

dissociated cells were gently passed through plastic tips and seeded into plastic flasks at a density of 10^7/300 cm^2 in Eagle's minimal essential medium, 0.3% $NaHCO_3$, 2 mM glutamine, 0.2% glucose, 10 μg/ml insulin, and 10% fetal calf serum, and maintained at 37°C with 10% CO_2, 90% air atmosphere. The subsequent medium replacement was renewed twice per week. After 10–14 days of culture, floating cells and weakly attached cells on the primary cultured cell layer were isolated by gently shaking the flask for 10 min. The resulting cell suspension was transferred to a petri dish (Falcon 1001, Lincoln Park, NJ) and then allowed to adhere at 37°C. The unattached cells were removed after 25 min, and microglial cells were isolated as strongly adhering cells. About 90% of these attached cells were positive for OX42 (Serotec Ltd., Bichester, UK), a marker for macrophage/microglal cell types.

The murine microglial cell line, 6-3, was established from neonatal C57BL/6J(H-2b) mice using a nonenzymatic and non-virus-transformed procedure [26]. The 6-3 cells closely resemble primary cultured microglia [26,27]. The 6-3 cells were cultured in Eagle's minimal essential medium, 0.3% $NaHCO_3$, 2 mM glutamine, 0.2% glucose, 10 μg/ml insulin, and 10% fetal calf serum, and then maintained at 37°C with 10% CO_2, 90% air atmosphere. The amount of 1 ng/ml mouse recombinant GM-CSF was supplemented in the culture medium to maintain the 6-3 cells because these cells stopped proliferating without it [26]. The culture media were renewed twice per week.

Fluorescence microscopy

After the 3-h treatment of NBD-labeled PS/PC liposomes (100 μM) or NBD-labeled PC liposomes (100 μM), primary cultured rat microglia were mounted on coverslips at a density of 1.0×10^4 cells/ml and were fixed with 4% paraformaldehyde for 30 min at room temperature. Afterward, the images were taken at an excitation of 470 nm and an emission of 530 nm using fluorescence microscopy (Leica Microsystems DMRB, Wetzlar, Germany).

TNF-α quantification

Primary cultured rat microglial cells were plated on 96-well tissue culture plates at 6×10^4 per 150 μl per well and then were incubated in the presence or absence of 50 μM Aβ25–35 peptides and/or 100 U/ml IFN-γ at 37°C. After 24 h, the collected media were assayed for TNF-α accumulation. TNF-α released into the culture medium was measured using a rat TNF-α enzyme-linked immunosorbent assay (ELISA) kit (Biosource International, Camarillo, CA) based on the quantitative "sandwich" enzyme immunosorbent technique. The assay was carried out according to the manufacturer's protocol. The sensitivity of this assay was 4 pg/ml.

RNA isolation and semiquantitative RT-PCR

Primary cultured rat microglial cells were plated on 60-mm dishes at a density of $1.0–1.5 \times 10^6$ cells per dish and then incubated with stimuli for 4 h. Cellular mRNA from microglia was extracted and purified by a QuickPrep micro mRNA purification kit (Amersham, UK) according to the manufacturer's protocol. The mRNA was subsequently reverse-transcribed to single-stranded complimentary DNA (cDNA) by SuperScrip II (Invitrogen, Carlsbad, CA) with the gene-specific primers described below. Aliquots of the cDNAs were then used in separate PCR amplifications using *Taq* polymerase (Invitrogen). To determine the optimal conditions which allowed the signal to be in the liner portion of the amplification curve, experiments were performed under conditions in which the cycle number and template concentrations were altered. A negative control lacking the template RNA or reverse transcriptase was included in each experiment. The cDNA products of the reverse transcription reaction were denatured at 94°C for 2 min and then PCR amplifications were carried out as follows: for TNF-α (primers, sense 5′-CCC AGA CCC TCA CAC TCA GAT-3′; antisense 5′-TTG TCC CTT GAA GAG AAC CTG-3′), 35 cycles of denaturation at 94°C for 15 s, annealing at 50°C for 30 s, and extension at 72°C for 30 s; for GAPDH (primers, sense 5′-ACC ACA GTC CAT GCC ATC AC-3′; antisense 5′-TCC ACC ACC CTG TTG CTG TA-3′) as an internal standard, 30 cycles of denaturation at 94°C for 30 s, annealing at 55°C for 30 s, and extension at 72°C for 30 s. PCR products were separated electrophoretically on 2% agarose gel and stained with 0.1 μg/ml ethidium bromide, and then were subsequently visualized under UV illumination. The results of a scanning densitometric analysis (NIH Image 1.62 and Adobe Photoshop 7.0) are expressed as the relative ratio of TNF-α/GAPDH.

NO quantification

The accumulation of NO_2^-, a stable end product, extensively used as an indicator of NO production by cultured cells, was assayed by the Griess reaction. Primary cultured rat microglial cells were plated on 96-well tissue culture plates at 6×10^4 per 150 μl per well and incubated in the presence or absence of 50 μM Aβ25–35 peptides and 100 U/ml IFN-γ at 37 °C. After 72 h, the cell-free supernatants were mixed with equal amounts of Griess reagent (Dojindo, Kumamoto, Japan). Samples were incubated at room temperature for 15 min and subsequently absorbance was read at 540 nm using a plate reader (Model 550; Bio-Rad, Richmond, CA).

Western blotting for the detection of inducible NO synthase (iNOS)

6-3 microglial cells were plated on 6-well tissue culture plates at a density of $1.0–1.5 \times 10^6$ cells per well and then incubated with stimuli for 12 h. Afterward, cells were washed with PBS (pH 7.4) and lysed with sodium dodecyl sulfate (SDS)-containing sample buffer. Proteins were separated in a 7.5% SDS-polyacrylamide gel and transferred onto nitrocellulose membrane. The membrane was incubated with 5% nonfat dry milk to block nonspecific binding. Subsequently, the membrane was incubated with iNOS antibodies (1:2000, Upstate, Lake Placid, NY) and β-actin antibodies (1:1000, Abcam, Cambridge, MA). The expression of iNOS was detected using an enhanced chemiluminescence

system (Amersham). The band intensity was quantified with a densitometric scanner (LAS 1000, Fujifilm, Tokyo, Japan).

ESR spectroscopy

ESR, together with the spin-trapping agent DEPMPO was employed to accurately detect the production of $^{\bullet}O_2^-$ by activated microglia. The 6-3 microglial cells were cultured on 12-well tissue culture plates at a density of 2×10^6 cells in 400 μl of culture medium per well. The 6-3 cells were primed by 100 U/ml IFN-γ for 16 h in the presence or absence of the pretreatment with PS/PC or PC liposomes for 1 h at 37°C. Afterward, the 6-3 cells were incubated at 37°C with or without 50 μM Aβ25–35 for 30 min before beginning the detection of ESR spectra. Cell suspensions (i.e., 5×10^6 cells/ml) in the culture medium containing 50 mM DEPMPO were transferred to a standard cell capillary, and the ESR measurements were performed at room temperature right after the incubation. The ESR spectra were obtained using a JES-RE1X ESR spectrometer (JEOL, Tokyo, Japan). The instrument conditions were set as follows: magnetic field = 336.85 ± 7.5 mT, modulation amplitude = 2000, modulation width = 0.1 mT, modulation frequency = 100 kHz, time constant = 0.1 s, microwave power = 10 mW, microwave frequency = 9430 MHz, and sweep time = 2 min.

Spin trapping in the xanthine/xanthine oxidase sysytem

Xanthine oxidase (0.1 U/ml) was incubated with 0.4 mM xanthine in phosphate buffer (PB) containing 2 mM DTPA and 20 mM DEPMPO in the presence or absence of 2 mM PS/PC liposomes or PC liposomes. Xanthine oxidase was added last to the mixture to start the reaction. The ESR spectra were recorded at room temperature on a JES-RE1X ESR spectrometer. The instrument conditions were set as follows: magnetic field = 336.85 ± 7.5 mT, modulation amplitude = 500, modulation width = 0.1 mT, modulation frequency = 100 kHz, time constant = 0.03 s, microwave power = 10 mW, microwave frequency = 9430 MHz, and sweep time = 1 min.

Statistics

Values are expressed as the means ± SE. All parameters were analyzed by a one-way analysis of variance (ANOVA) followed by Fisher's PLSD post hoc test for specific comparisons. The significance was established at a level of $P < 0.05$.

Results

Confirmation of microglial phagocytosis of PS/PC liposomes

First, in order to confirm that the prepared liposomes are certainly engulfed by microglia, we treated primary cultured rat microglia with NBD-labeled PS/PC liposomes or NBD-labeled PC liposomes. After 3 h of treatment, the microglia were fixed with 4% PFA and examined by fluorescence microscopy. The fluorescent images were merged with the corresponding phase-contrast images. As shown in Fig. 1A, well-defined microglial cytoplasm was observed to fill with fluorescently labeled PS/PC liposomes (green). In contrast, few PC liposomes labeled with the fluorescence were observed in the microglial cytoplasm (Fig. 1B). These findings indicate that PS/PC liposomes, but not PC liposomes, were phagocytosed by microglia.

Effect of PS/PC liposomes on the TNF-α production by Aβ/IFN-γ-activated microglia

We next investigated the effect of PS/PC liposomes on the TNF-α production by Aβ/IFN-γ-activated microglia. The incubation of primary cultured rat microglia with 50 μM Aβ25–35 combined with 100 U/ml IFN-γ for 24 h resulted in significant increases in the accumulation of TNF-α, whereas neither Aβ25–35 alone nor IFN-γ alone were able to activate the microglia to release TNF-α (Fig. 2A). The massive increase was significantly reduced by the pretreatment with PS/PC liposomes for 1 h in a dose-dependent manner (Fig. 2A).

In line with the results on the protein levels, the suppressive effect of PS/PC liposomes on the expression of mRNA

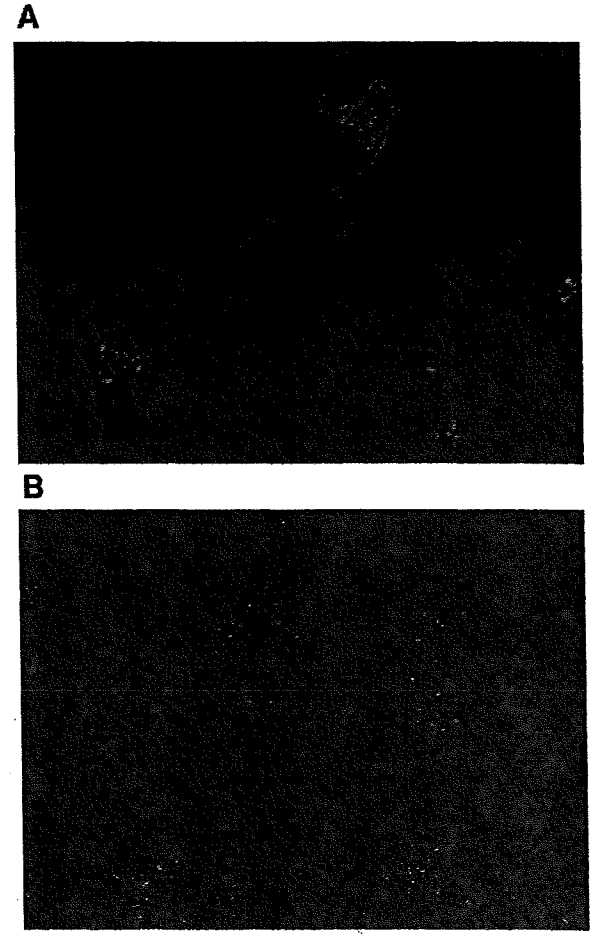

Fig. 1. Microglial phagocytosis of PS/PC liposomes. A typical fluorescence microphotograph showing phagocytosis of NBD-labeled PS/PC liposomes (green) by primary cultured rat microglia. The fluorescent image was merged with the corresponding phase-contrast image.

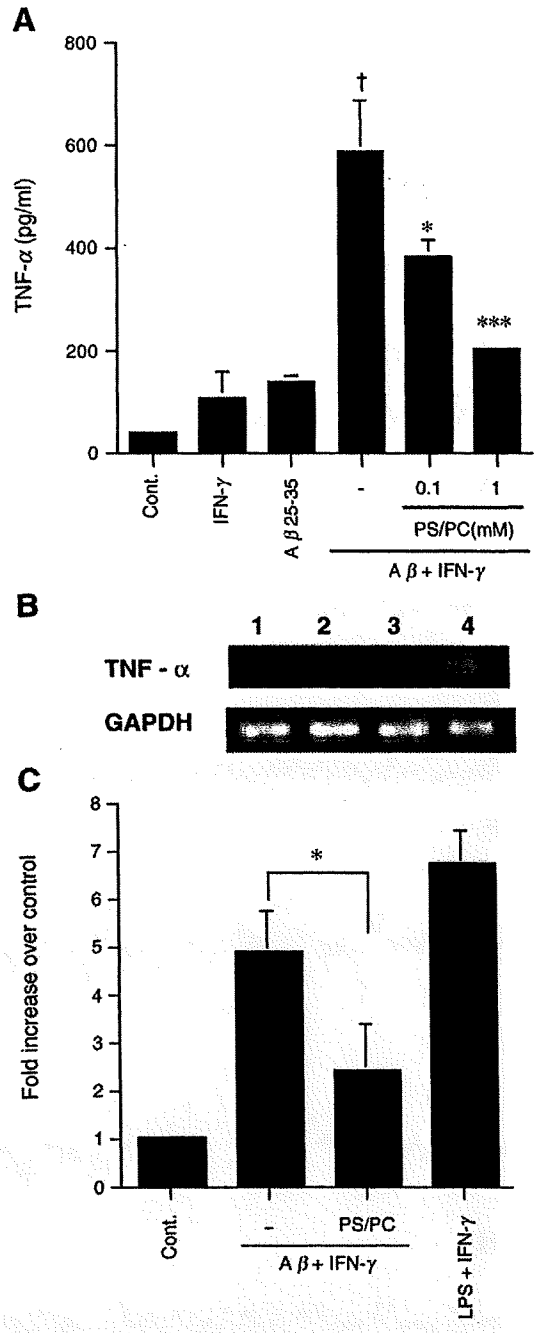

Fig. 2. Effect of PS/PC liposomes on the TNF-α production by Aβ/IFN-γ-activated microglia. (A) Primary cultured rat microglia were incubated with 50 μM Aβ25–35 and/or 100 U/ml IFN-γ at 37°C with or without pretreatment of PS/PC liposomes for 1 h. After 24 h, the collected media were assayed for TNF-α accumulation using ELISA. Data are the mean values ± SE (n=3). †P<0.0001, compared with control. *P<0.05, ***P<0.001, compared with Aβ25–35 + IFN-γ. (B) A representative RT-PCR analysis of the expression of mRNA encoding TNF-α in primary cultured rat microglia incubated with stimuli for 4 h with or without pretreatment of 1 mM PS/PC liposomes for 1 h. The administration of 10 ng/ml LPS combined with 100 U/ml IFN-γ was conducted as a positive control for the expression of TNF-α mRNA. Lane 1, control (medium); 2, Aβ25–35 + IFN-γ; 3, Aβ25–35 + IFN-γ + PS/PC liposomes; 4, LPS + IFN-γ. (C) Individual TNF-α mRNA levels were normalized to the corresponding levels of the mRNA encoding GAPDH. The results are expressed as the fold increase in the ratio of treated cell groups over the control. Data are the mean values ± SE (n = 3). *P < 0.05.

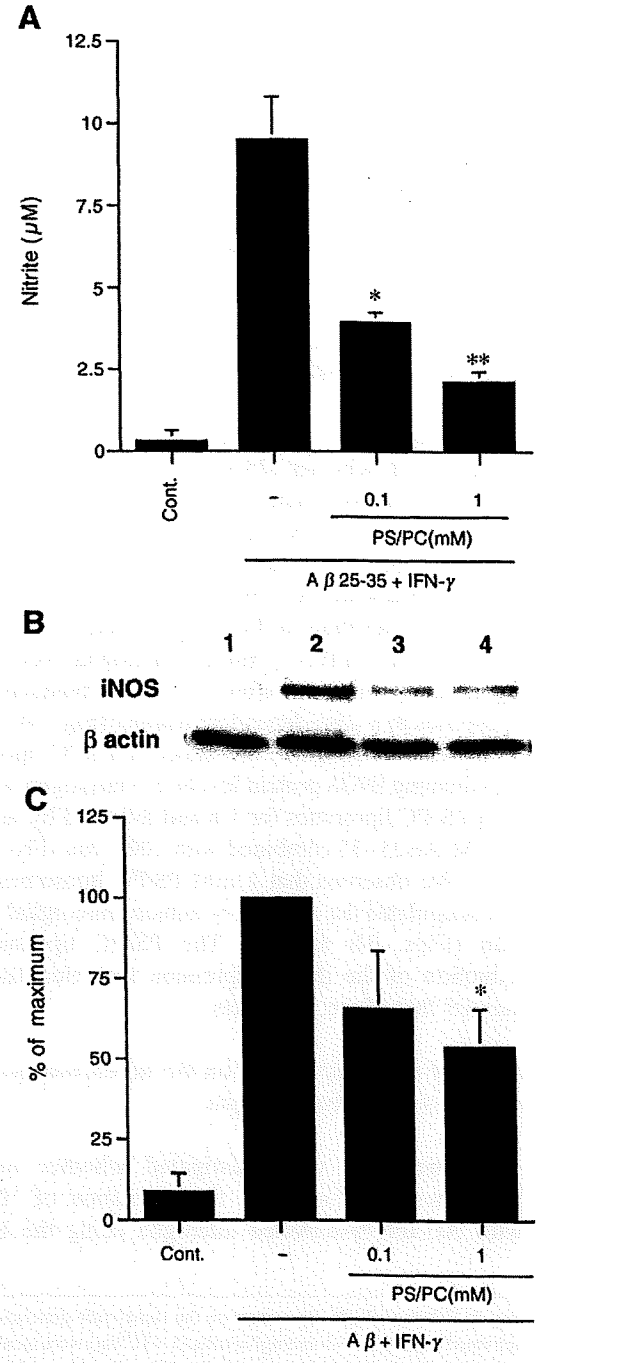

Fig. 3. Effect of PS/PC liposomes on the NO production by Aβ/IFN-γ-activated microglia. (A) Primary cultured rat microglial cells were incubated with 50 μM Aβ25–35 and 100 U/ml IFN-γ at 37°C with or without pretreatment of 1 mM PS/PC liposomes for 1 h. After 72 h, the collected media were assayed for NO accumulation using the Griess reaction. Data are the mean values ± SE. (n = 3). *P < 0.05, **P < 0.01, compared with Aβ25–35 + IFN-γ. (B) Representative Western blotting analysis of the expression of iNOS in 6-3 microglial cells incubated with Aβ25–35 + IFN-γ for 12 h with or without pretreatment of PS/PC liposomes for 1 h. Lane 1, control (medium); 2, Aβ25–35 + IFN-γ, 3, Aβ25–35 + IFN-γ + PS/PC liposomes (0.1 mM); 4, Aβ25–35 + IFN-γ + PS/PC liposomes (1 mM). (C) Individual iNOS expression levels were normalized to the corresponding levels of β-actin. The results are expressed as the percentage of the maximum levels (i.e., Aβ25–35 + IFN-γ). Data are the mean values ± SE. (n = 3). *P < 0.05 compared with Aβ25–35 + IFN-γ.

encoding TNF-α was also demonstrated by semiquantitative RT-PCR analyses. The levels of TNF-α mRNA isolated from primary cultured rat microglia incubated with 50 μM Aβ25–35 and 100 U/ml IFN-γ at 37°C for 4 h expressed approximately a fivefold rise over the nonstimulated control (Fig. 2C). The levels of increased TNF-α mRNA expression were significantly inhibited by the pretreatment with 1 mM PS/PC liposomes for 1 h to approximately two-to threefold levels of the control (Fig. 2C). The administration of 10 ng/ml LPS combined with 100 U/ml IFN-γ was conducted as a positive control for the expression of TNF-α mRNA.

Effect of PS/PC liposomes on the NO production by Aβ/IFN-γ-activated microglia

Subsequently, employing the Griess reaction assay, we investigated whether PS/PC liposomes also decrease the synthesis of NO, which is a potentially proinflammatory molecule and a tally of $^{\bullet}O_2^-$ for $ONOO^-$ formation. The incubation of primary cultured rat microglia with 50 μM Aβ25–35 combined with 100 U/ml IFN-γ at 37°C for 72 h resulted in a significant elevation in the accumulation of NO (Fig. 3A). As expected, the Aβ/IFN-γ-induced microglial NO production was significantly inhibited after 1 h of pretreatment with PS/PC liposomes in a dose-dependent manner (Fig. 3A).

We also investigated the effect of PS/PC liposomes on the NO-forming iNOS protein levels. 6-3 microglia were pretreated with PS/PC liposomes for 1 h and followed by incubation with 50 μM Aβ25–35 combined with 100 U/ml IFN-γ at 37 °C for 12 h. We observed that 1 mM PS/PC liposomes significantly downregulated the Aβ/IFN-γ-induced microglial iNOS expression (Figs. 3B and C). The PS/PC liposomes-mediated reduction of the iNOS expression was elucidated to closely parallel that of the NO levels.

Effect of PS/PC liposomes on the superoxide generation by Aβ/IFN-γ-activated microglia

Furthermore, we investigated whether or not PS/PC liposomes could suppress the generation of $^{\bullet}O_2^-$ associated with Aβ/IFN-γ-activated microglia using the ESR spin-trap

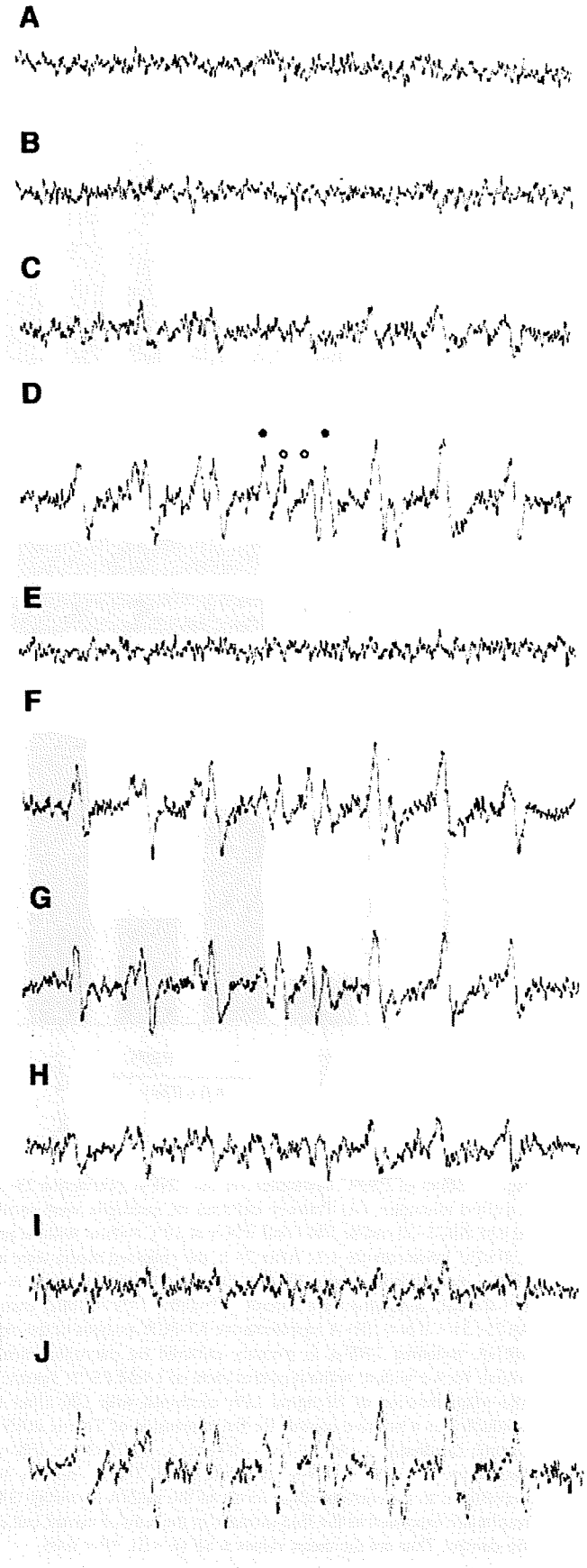

Fig. 4. Effect of PS/PC liposomes on the superoxide generation by Aβ/IFN-γ-activated microglia. 6-3 microglial cells (5×10^6/ml) were incubated with 100 U/ml IFN-γ for 16 h and 50 μM Aβ25–35 for 30 min at 37°C with or without pretreatment of PS/PC or PC liposomes for 1 h. The ESR spectra were then recorded in the presence of 50 mM DEPMPO at room temperature. (A) ESR spectra obtained from 50 μM Aβ25–35 peptide alone (cell free). (B) ESR spectra of DEPMPO adducts obtained from nonstimulated microglia. (C) ESR spectra of DEPMPO adducts obtained from the microglia stimulated by IFN-γ alone. (D) ESR spectra of DEPMPO adducts obtained from Aβ25–35/IFN-γ-activated microglia. Open and closed circles represent the measured signal peaks of DEPMPO-OH and DEPMPO-OOH adducts, respectively. (E) The same as D, but with the addition of SOD (160 μg/ml). (F) The same as D, but with the addition of catalase (280 μg/ml). (G) The same as D, but after pretreatment with PS/PC liposomes (0.5 mM) for 1 h. (H) The same as D, but after pretreatment with PS/PC liposomes (1 mM) for 1 h. (I) The same as D, but after pretreatment with PS/PC liposomes (2 mM) for 1 h. (J) The same as D, but after pretreatment with PC liposomes (2 mM) for 1 h.

technique with DEPMPO. Because several previous studies have reported spontaneously generated free radicals associated with high concentrations of Aβ peptides (i.e., millimolar order) [28,29], we beforehand confirmed that the concentrations of Aβ peptides used in this study (i.e., 50 μM) had no potency to generate $^{\bullet}O_2^-$ by itself (Fig. 4A).

In the preparations of nonstimulated 6-3 microglial cells, no signals were obtained (Fig. 4B). Microglial cells stimulated by 100 U/ml IFN-γ alone in the presence of 50 mM DEPMPO showed the weak signals whose spectra can hardly be clarified (Fig. 4C). Microglial cells stimulated by 50 μM Aβ25–35 combined with 100 U/ml IFN-γ in the presence of 50 mM DEPMPO showed prominent signals whose spectra consisted of a linear combination of a characteristic 12-line spectrum corresponding to $^{\bullet}O_2^-$ spin adduct DEPMPO-OOH and an 8-line spectrum corresponding to $^{\bullet}OH$ spin adduct DEPMPO-OH (Fig. 4D). Computer simulation confirmed DEPMPO-OOH with hyperfine splittings a_N=13.22 G, a^{β}_H=10.962 G, a_p=50.281 G, a^{γ}_H=0.666 G and DEPMPO-OH with hyperfine splittings a_N=12.723 G, a_H=13.124 G, a_p=51.119 G. To further confirm the original species of the spin adduct generated by Aβ/IFN-γ-activated microglia, SOD (160 μg/ml) or catalase (280 μg/ml) was also treated. The ESR signal intensity substantially decreased by SOD (Fig. 4E), not by catalase (Fig. 4F). These results indicate that the spin adducts originated from the $^{\bullet}O_2^-$ radical, but not from the $^{\bullet}OH$ radical which is derived from H_2O_2. As well as an inhibitory effect of PS/PC liposomes on the TNF-α and NO production, pretreatment with PS/PC liposomes for 1 h considerably decreased the of $^{\bullet}O_2^-$ generation by Aβ/IFN-γ-activated microglia in a dose-dependent manner (Figs. 4G, H, and I). Because PC has been demonstrated to presumably act as a membrane perturber, thus reducing the production of ROS in LPS/PMA-activated monocytes [9] and in LPS/PMA-activated microglia [30], we also evaluated the effect of PC liposomes on the generation of $^{\bullet}O_2^-$ associated with Aβ/IFN-γ-activated microglia. In contrast to PS/PC liposomes, pretreatment with 2 mM PC liposomes for 1 h did not mimic the inhibitory effect of PS/PC liposomes on $^{\bullet}O_2^-$ generation of by Aβ/IFN-γ-activated microglia at all (Fig. 4J).

Effect of PS/PC liposomes on the $^{\bullet}O_2^-$ generation in the xanthine/xanthine oxidase system

To confirm whether or not the liposomes per se scavenge $^{\bullet}O_2^-$, we measured the $^{\bullet}O_2^-$ production in the xanthine/xanthine oxidase system in the presence or absence of PS/PC liposomes using ESR monitoring with a spin-trap DEPMPO. Fig. 5A shows the typical ESR spectra consisting of DEPMPO-OOH and DEPMPO-OH in the xanthine/xanthine oxidase system. The formation of these spin adducts via trapping $^{\bullet}O_2^-$ was confirmed by experiments in which SOD (160 μg/ml) was added before xanthine oxidase and ESR signals were completely quenched (data not shown), while catalase (280 μg/ml) was added, in which ESR signals were not quenched at all (data not shown). The ESR spectra in the presence of either 2 mM PS/PC liposomes were found to be essentially the same as those shown in Fig. 5A, thus indicating that PS/PC liposomes have no scavenging effect on $^{\bullet}O_2^-$, but they do have an inhibitory effect on the $^{\bullet}O_2^-$ generating system in the microglia (Fig. 5B).

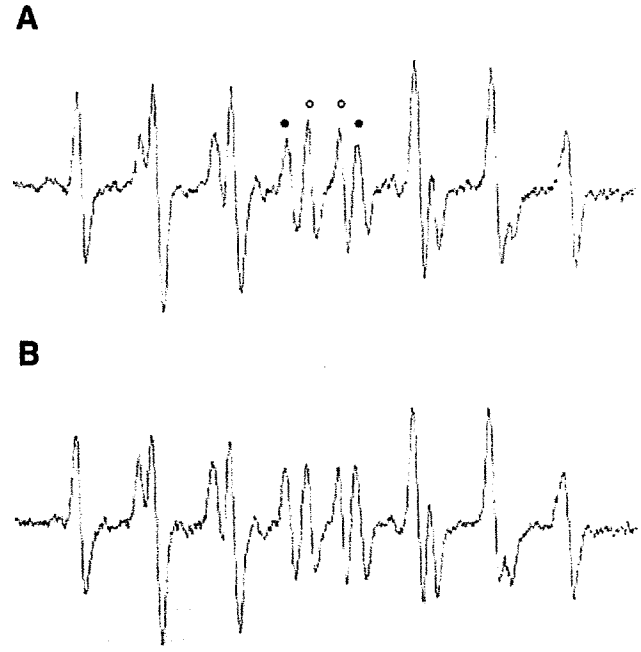

Fig. 5. Effect of PS/PC liposomes on the superoxide generation in the xanthine/xanthine oxidase system. The system contained 0.4 mM xanthine, 2 mM DTPA, and 20 mM DEPMPO in PB in the presence or absence of 2 mM PS/PC liposomes or PC liposomes. Xanthine oxidase (0.1 U/ml) was added last to the mixture in order to start the reaction. (A) ESR spectra of DEPMPO adducts obtained in the xanthine/xanthine oxidase system. Open and closed circles represent the measured signal peaks of the DEPMPO-OH and DEPMPO-OOH adducts, respectively. (B) The same as A, but in the presence of 2 mM PS/PC liposomes.

Discussion

During phagocytosis, an abrupt $^{\bullet}O_2^-$ formation called a respiratory burst occurs through activation of nicotinamide adenine diphosphate reduced form (NADPH) oxidase in phagocytes such as macrophage, neutrophils, and microglia. The $^{\bullet}O_2^-$ radical is a precursor of the microbicidal oxidants and it thus plays a crucial role in the host defense [31]. $^{\bullet}O_2^-$ is also involved in the AD pathophysiology associated with microglia-mediated neuroinflammation and oxidative stress because of $^{\bullet}O_2^-$ derivative products such as $^{\bullet}OH$ and $ONOO^-$, both of which are highly reactive and capable of exerting neurotoxicity. Especially, increasing attention has recently been paid to $ONOO^-$ as a major factor for neurotoxicity in AD pathophysiology [7,8]. Shimohama et al. have shown that the activity of NADPH oxidase is elevated in AD brains [32] and several in vitro studies have shown that Aβ activates NADPH oxidase in different cell types, thereby inducing $^{\bullet}O_2^-$ production. Specifically, Aβ25–35 has been shown to activate NADPH oxidase in human monocytes and neutrophils [33] while also inducing $^{\bullet}O_2^-$ generation in both rat microglia and human monocytes [34], and by rat peritoneal macrophages [35]. All of these studies,

however, indirectly measured the Aβ-induced $^{\bullet}O_2^-$ generation using the $^{\bullet}O_2^-$ dependent SOD-sensitive reduction of cytochrome *c*. Therefore, we directly measured the $^{\bullet}O_2^-$ generation by Aβ/IFN-γ-activated microglia using ESR with the spin-trap technique to evaluate the effect of PS/PC liposomes on microglial $^{\bullet}O_2^-$ production.

The DEPMPO is an appropriate spin-trapping agent for cell-generated $^{\bullet}O_2^-$ detection because of its stability and capability of differentiating between $^{\bullet}O_2^-$ and $^{\bullet}OH$ [36,37]. Aβ/IFN-γ-activated microglia gave rise to ESR spectra consisting of a linear combination of $^{\bullet}O_2^-$ spin adduct DEPMPO-OOH and spin adduct DEPMPO-OH. The formation of spin adducts was totally quenched by SOD but not by catalase, thus indicating that H_2O_2, which is reduced to $^{\bullet}OH$ by the Fenton reaction in the presence of Fe^{2+} or Zn^{2+}, was not a significant reactant in the formation of the observed radial signals. Moreover, the DEPMPO-OH appears to be generated by a spontaneous reduction of DEPMPO-OOH, not from H_2O_2-derived $^{\bullet}OH$ [37]. Although the noted property of DEPMPO made it possible to detect a sufficient amount of $^{\bullet}O_2^-$ to evaluate the effect of PS/PC liposomes on microglial activation in the present study, DEPMPO has recently been shown to trap $^{\bullet}O_2^-$ inefficiently in the presence of NO because the rate of the reaction between NO with $^{\bullet}O_2^-$ is faster than the rate of the reaction between DEPMPO with $^{\bullet}O_2^-$ [38]. Accordingly, the proper amount of microglial $^{\bullet}O_2^-$ generation after 16 h treatment with Aβ/IFN-γ may be larger than that demonstrated by our data under the experimental conditions supposed to induce iNOS in microglial cells.

Our data demonstrated that PS/PC liposomes have an inhibitory effect on the Aβ/IFN-γ-induced microglial production of inflammatory molecules such as TNF-α, NO, and $^{\bullet}O_2^-$, and they thus presumably prevent the subsequent formation of $ONOO^-$. Accordingly, PS/PC liposomes appear to have both neuroprotective and antioxidative properties through the inhibition of microglial activation and to be a potentially useful treatment for microglial activation-mediated neurodegenerative diseases including AD. The exact mechanism of PS/PC liposomes to suppress inflammatory activation of microglia has not yet been elucidated. De Simone et al. have indicated that the inhibitory effect of PS-containing liposomes on microglial activation is not restricted to a specific stimulant-evoked signal (s) [13]. Indeed, we previously have demonstrated that PS/PC liposomes can inhibit LPS/IFN-γ-induced microglial activation [30] as well as Aβ/IFN-γ-induced microglial activation. Consequently, PS/PC liposomes may affect various signal pathways associated with inflammatory responses in activated microglia. Ajmone-Cat et al. have shown that PS/PC-containing liposomes inhibited the phosphorylation of p38 mitogen-activated protein kinase (MAPK) and delayed that of cAMP responding element binding protein in LPS-activated microglia [39]. Because phosphorylation of p38 MAPK has been shown to mediate the signal pathway reacting for inflammatory stimulants and result in gene induction of TNF-α and NO synthase in microglia [40], the PS/PC liposomes-induced inhibition of p38 MAPK phosphorylation in activated microglia appears to suppress, at least partially, TNF-α and NO generation. Alternatively, it is also possible that the decrease in the TNF-α and NO production is a direct consequence of both decreased $^{\bullet}O_2^-$ derived ROS generation and decreased redox signaling. In support of this, there is increasing evidence that ROS can function as a second messenger to regulate several downstream molecules such as MAPKs and nuclear factor-κB (NF-κB) [41]. Indeed, it has been demonstrated that activation of NF-κB, upon which TNF-α and iNOS expression is at least partially dependent, is redox sensitive [42]. Furthermore, ROS has been reported to mediate proinflammatory signaling in LPS-activated microglia and thus amplify TNF-α production [22]. Accordingly, through directly decreasing $^{\bullet}O_2^-$ derived ROS generation, PS/PC liposomes may act indirectly to limit a wide variety of subsequent inflammatory pathways. Due to the notable role of $^{\bullet}O_2^-$ as an inflammatory enhancer as noted above, a future study investigating the effect of PS/PC liposomes on $^{\bullet}O_2^-$ forming NADPH oxidase in Aβ/IFN-γ-activated microglia is called for to clarify the $^{\bullet}O_2^-$ inhibition mechanism of PS/PC liposomes.

There is increasing evidence that TNF-α can be neuroprotective as well as neurotoxic [43]. Although the precise function of TNF-α in the pathogenesis of AD remains unclear, this cytokine might be a key mediator in modulating the microglial functions in response to Aβ [44]. In addition, a number of infiltrating T cells have been shown to increase in the brain of AD [45] and the immune cells of AD patients have the potency for overproduction of IFN-γ [46]. According to such evidence, our experimental method using IFN-γ thus seems to be consistent with the pathophysiologic microenvironment in the AD brain.

Small et al. suggested that because neuronal loss does not account, by itself, for the properties of the amnesia characteristics of AD, more attention should be paid to the effect of Aβ peptides on the synaptic function rather than on neuronal death [47]. Accordingly, the effect of PS/PC liposomes on the synaptic dysfunction caused by Aβ-induced microglial activation also needs to be confirmed in future in vivo studies, regardless PS-containing liposomes have been reported to prevent the LPS-induced impairment of LTP [17].

The total lipid concentration such as the 1 mM PS/PC liposomes used in this study certainly seems to be high. Borisenko et al., however, have suggested that phagocytes have a sensitivity threshold for PS externalized on the target cell surface which thus allows for the reliable recognition and distinction between normal cells with low amounts of externalized PS and apoptotic cells with remarkably elevated PS levels [48]. They estimated that, using the liposomes containing PS and PC (1:1), the absolute amount of PS required for phagocytosis by 5×10^4 macrophages (the threshold of macrophage sensitivity) was 7 pmol. This value of the PS amount for 10^6 macrophages (i.e., 140 pmol) approximates to the normalized value of the PS amount for 10^6 microglial cells (i.e., 60 pmol), and this value was found to be quite effective in our study. Taken together, these findings suggest that microglial cells also seem to require a relatively high phospholipid concentration to recognize PS/PC liposomes as apoptotic cells. Accordingly, new techniques to ameliorate the stability of PS/PC liposomes and reduce the effective phospholipids concentration are required for future in vivo studies.

Acknowledgments

This study was supported by a Grant-in-Aid for the Creation of Innovations through Business-Academic-Public Sector Corporation of Japan (HN), a Grant-in-Aid (15082204) (H.N.) and a Grant-in-Aid (15591230) (A.M.) for Scientific Research on Priority Areas from the Ministry of Education, Science and Culture, Japan, and a grant from Inogashira Hospital (S.H.). We thank Prof. Yukihiro Shoyama and Dr. Satoshi Morimoto, Department of Plant Resources Regulation, Graduate School of Pharmaceutical Sciences, Kyushu University, for their valuable technical advice regarding the preparation of the liposomes.

References

[1] Itagaki, S.; McGeer, P. L.; Akiyama, H.; Zhu, S.; Selkoe, D. Relationship of microglia and astrocytes to amyloid deposits of Alzheimer's disease. *J. Neuroimmunol.* **24**:173–182; 1989.

[2] Eikelenboom, P.; Bate, C.; Van Gool, W. A.; Hoozemans, J. J. M.; Rozemuller, J. M.; Veerhuis, R.; Williams, A. Neuroinflammation in Alzheimer's disease and prion disease. *Glia* **40**:232–239; 2002.

[3] Combs, C. K.; Karlo, J. C.; Kao, S. C.; Landreth, G. E. β-Amyloid stimulation of microglia, and monocytes results in TNF-α-dependent expression of inducible nitric oxide synthase and neuronal apoptosis. *J. Neurosci.* **21**:1179–1188; 2001.

[4] Hashioka, S.; Monji, A.; Ueda, T.; Kanba, S.; Nakanishi, H. Amyloid-beta fibril formation is not necessarily required for microglial activation by the peptides. *Neurochem. Int.* **47**:369–376; 2005.

[5] Meda, L.; Cassatella, M. A.; Szendrei, G. I.; Otvos Jr., L.; Baron, P.; Villalba, M.; Ferrari, D.; Rossi, F. Glial activation in Alzheimer's disease: the role of Aβ and its related proteins. *Nature* **374**:647–650; 1995.

[6] Qin, L.; Liu, Y.; Cooper, C.; Liu, B.; Wilson, B.; Hong, J. S. Microglia enhance β-amyloid peptide-induced toxicity in cortical and mesencephalic neurons by producing reactive oxygen species. *J. Neurochem.* **83**: 973–983; 2002.

[7] Xie, Z.; Wei, M.; Morgan, T. E.; Fabrizio, P.; Han, D.; Finch, C. E.; Longo, V. D. Peroxynitrite mediates neurotoxicity of amyloid β-peptides 1-42 and lipopolysaccharide-activated microglia. *J. Neurosci.* **22**:3484–3492; 2002.

[8] Smith, M. A.; Richey Harris, P. L.; Sayre, L. M.; Beckman, J. S.; Perry, G. Widespread peroxynitrite-mediated damage in Alzheimer's disease. *J. Neurosci.* **17**:2653–2657; 1997.

[9] Tonks, A.; Parton, J.; Tonks, A. J.; Morris, R. H.; Finall, A.; Jones, K. P.; Jackson, S. K. Surfactant phospholipid DPPC downregulates monocyte respiratory burst via modulation of PKC. *Am. J. Physiol. Lung Cell Mol. Physiol.* **288**:1070–1080; 2005.

[10] Fadok, V. A.; Bratton, D. L.; Henson, P. M. Phagocyte receptor for apoptotic cells: recognition, uptake, and consequences. *J. Clin. Invest.* **108**:957–962; 2001.

[11] Fadok, V. A.; Bratton, D. L.; Konowal, A.; Freed, P. W.; Westcott, J. Y.; Henson, P. M. Macrophages that have ingested apoptotic cells in vitro inhibit proinflammatory cytokine production through autocrine/paracrine mechanism involving TGF-β PGE2, and PAF. *J. Clin. Invest.* **101**: 890–898; 1998.

[12] Fadok, V. A.; Bratton, D. L.; Rose, D. M.; Pearson, A.; Ezekewitz, R. A. A receptor for phosphatidylserine-specific clearance of apoptotic cells. *Nature* **405**:85–90; 2000.

[13] De Simone, R.; Ajmone-Cat, M. A.; Nicolini, A.; Minghetti, L. J. Expression of phosphatidylserine receptor and down-regulation of proinflammatory molecule producton by its natural ligand in rat microglial cultures. *Neuropathol. Exp. Neurol.* **61**:237–244; 2002.

[14] Zhang, J.; Fujii, S.; Wu, Z.; Hashioka, S.; Tanaka, Y.; Shiratsuchi, A.; Nakanishi, Y.; Nakanishi, H. Involvement of COX-1 and up-regulated prostaglandin E synthases in phosphatidylserine liposome-induced prostaglandin E2 production by microglia. *J. Neuroimmunol.* **172**:112–120; 2005.

[15] McDaniel, M. A.; Maier, S. F.; Einstein, G. O. "Brain-specific" nutrients: a memory cure? *Nutrition* **19**:957–975; 2003.

[16] Suzuki, S.; Yamatoya, H.; Sakai, M.; Kataoka, A.; Furushiro, M.; Kudo, S. Oral administration of soybean lecithin transphosphatidylated phosphatidylserine improves memory impairment in aged rats. *J. Nutr.* **131**: 2951–2956; 2001.

[17] Nolan, Y.; Martin, D.; Campbell, V. A.; Lynch, M. A. Evidence of a protective effect of phosphatidylserine-containing liposomes on lipopolysaccharide-induced impairment of long-term potentiation in the rat hippocampus. *J. Neuroimmunol.* **151**:12–23; 2004.

[18] Delwaide, P. J.; Gyselynck-Mambourg, A. M.; Hurlet, A.; Ylieff, M. Double-blind randomized controlled study of phosphatidylserine in senile demented patients. *Acta Neurol. Scand.* **73**:136–140; 1986.

[19] Cenacchi, T.; Bertoldin, T.; Farina, C.; Fiori, M. G.; Crepaldi, G. (and participating investigators). Cognitive decline in the elderly: a double-blind, placebo-controlled multicenter study on efficacy of phosphatidylserine administration. *Aging Clin. Exp. Res.* **5**:123–133; 1993.

[20] Navarro-Antolin, J.; Lopez-Munoz, M. J.; Soria, J.; Lamas, S. Superoxide limits cyclosporine-A-induced formation of peroxynitrite in endothelial cells. *Free Radic. Biol. Med.* **32**:702–711; 2002.

[21] Possel, H.; Noack, H.; Keilhoff, G.; Wolf, G. Life imaging of peroxynitrite in rat microglial and astroglial cells: role of superoxide and antioxidants. *Glia* **38**:339–350; 2002.

[22] Qin, L.; Liu, Y.; Wang, T.; Wei, S. J.; Block, M. L.; Wilson, B.; Liu, B.; Hong, J. S. NADPH oxidase mediates lipopolysaccharide-induced neurotoxicity and proinflammatory gene expression in activated microglia. *J. Biol. Chem.* **279**:1415–1421; 2004.

[23] Chang, R. C. C.; Rota, C.; Glover, R. E.; Mason, R. P.; Hong, J. S. A novel effect of an opioid receptor antagonist, naloxone, on the product of reactive oxygen species by microglia: a study by electron paramagnetic resonance spectroscopy. *Brain Res.* **854**:224–229; 2000.

[24] Nishikawa, K.; Arai, H.; Inoue, K. Scavenger receptor-mediated uptake and metabolism of lipid vesicles containing acidic phospholipids by mouse peritoneal macrophages. *J. Biol. Chem.* **256**:5226–5231; 1990.

[25] Sastradipura, D. F.; Nakanishi, H.; Tsukuba, T.; Nishishita, K.; Sakai, H.; Kato, Y.; Gtow, T.; Uchiyama, Y.; Yamamoto, K. Identification of cellular component involved in processing of cathepsin E in primary cultures of rat microglia. *J. Neurochem.* **70**:2045–2056; 1998.

[26] Kanzawa, T.; Sawada, M.; Kato, K.; Yamamoto, K.; Mori, H.; Tanaka, R. Differentiated regulation of allo-antigen presentation by different types of murine microglial cell lines. *J. Neurosci. Res.* **62**:383–388; 2000.

[27] Sawada, M.; Imai, F.; Suzuki, H.; Hayakawa, M.; Kanno, T.; Nagatsu, T. Brain-specific gene expression by immortalized microglial cell-mediated gene transfer in the mammalian brain. *FEBS Lett.* **433**:37–40; 1998.

[28] Monji, A.; Utsumi, H.; Ueda, T.; Imoto, T.; Yoshida, I.; Hashioka, S.; Tashiro, K.; Tashiro, N. The relationship between the aggregational state of the amyloid-βpeptides and free radical generation by the peptides. *J. Neurochem.* **77**:1425–1432; 2001.

[29] Varadarajan, S.; Yatin, S.; Aksenova, M.; Jahanshahi, F.; Butterfield, D. A. Review: Alzheimer's amyloid β-peptide-associated free radical oxidative stress and neurotoxicity. *J. Struct. Biol.* **130**:184–208; 2000.

[30] Hashioka, S.; Han, Y. H.; Fujii, S.; Kato, T.; Monji, A.; Utsumi, H.; Sawada, M.; Nakanishi, H.; Kanba, S.; Phospholipids modulate superoxide and nitric oxide production by lipopolysaccharide and phorbol 12-myristate-13-acetate-activated microglia, Neurochem, Int. in press. doi:10.1016/j.neuint.2006.10.006.

[31] Ueyama, T.; Lennartz, M. R.; Noda, Y.; Kobayashi, T.; Shirai, Y.; Rikitake, K.; Yamasaki, T.; Hayashi, S.; Sakai, N.; Seguchi, H.; Sawada, M.; Sumimoto, H.; Saito, N. Superoxide production at phagosomal cup/phagosome through beta I protein kinase C during Fc gamma R-mediated phagocytosis in microglia. *J. Immunol.* **173**:4582–4589; 2004.

[32] Shimohama, S.; Tanio, H.; Kawakami, N.; Okamura, N.; Kodama, H.; Yamaguchi, T.; Nunomura, A.; Chiba, S.; Perry, G.; Smith, M. A.; Fujimoto, S. Activation of NADPH oxidase in Alzheimer's disease brains. *Biochem. Biophys. Res. Commun.* **273**:5–9; 2000.

[33] Bianca, V. D.; Dusi, S.; Bianchini, E.; Pra, I. D.; Rossi, F. Beta amyloid activates the O_2 forming NADPH oxidase in microglia,monocytes,and

neutrophils. A possible inflammatory mechanism of neuronal damage in Alzheimer's disease. *J. Biol. Chem.* **274**:15493–15499; 1999.

[34] McDonald, D. R.; Brunden, K. R.; Landreth, G. E. Amyloid fibrils activate tyrosine kinase-dependent signaling and superoxide production in microglia. *J. Neurosci.* **17**:2284–2294; 1997.

[35] Klegeris, A.; McGeer, P. L. β-Amyloid protein enhances macrophage production of oxygen free radicals and glutamate. *J. Neurosci. Res.* **49**:229–235; 1997.

[36] Shi, H.; Timmins, G.; Monske, M.; Burdick, A.; Kalyanaraman, B.; Liu, Y.; Clement, J. L.; Burchiel, S.; Liu, K. J. Evaluation of spin trapping agents and trapping conditions for detection of cell-generated reactive oxygen species. *Arch. Biochem. Biophys.* **437**:59–68; 2005.

[37] Mojovic, M.; Vuletic, M.; Bacic, G. G. Detection of oxygen-centered radicals using EPR spin-trap DEPMPO: the effect of oxygen. *Ann. N.Y. Acad. Sci.* **1048**:471–475; 2005.

[38] Pignitter, M.; Gorren, A. C.; Nedeianu, S.; Schmidt, K.; Mayer, B. Inefficient spin trapping of superoxide in the presence of nitric-oxide: implications for studies on nitric-oxide synthase uncoupling. *Free Radic. Biol. Med.* **41**:455–463; 2006.

[39] Ajmone-Cat, M. A.; De Simone, R.; Nicolini, A.; Minghetti, L. J. Effects of phosphatidylserine on p38 mitogen activated protein kinse, cyclic AMP responding element binding protein and nuclear factor-kB activation in resting and activated microglial cells. *J. Neurochem.* **84**:413–416; 2003.

[40] Koistinaho, M.; Koistinaho, J. Role of p38 and p44/42 mitogen-activated protein kinases in microglia. *Glia* **40**:175–183; 2002.

[41] Esposito, F.; Ammendola, R.; Faraonio, R.; Russo, T.; Cimino, F. Redox control of signal transduction, gene expression and cellular senescence. *Neurochem. Res.* **29**:617–628; 2004.

[42] Kaul, N.; Forman, H. J. Activation of NF kappa B by the respiratory burst of macrophages. *Free Radic. Biol. Med.* **21**:401–405; 1996.

[43] Suzuki, T.; Hide, I.; Ido, K.; Kohsaka, S.; Inoue, K.; Nakata, Y. Production and release of neuroprotective tumor necrosis factor by P2X7 receptor-activated microglia. *J. Neurosci.* **24**:1–7; 2004.

[44] Meda, L.; Baron, P.; Scarlato, G. Glial activation in Alzheimer's disease: the role of Aβ and its related proteins. *Neurobiol. Aging* **22**:885–893; 2001.

[45] Togo, T.; Akiyama, H.; Iseki, E.; Kondo, H.; Ikeda, K.; Kato, M.; Oda, T.; Tuchiya, K.; Kosaka, K. Occurrence of T cells in the brain of Alzheimer's disease and other neurological diseases. *J. Neuroimmunol.* **124**:83–92; 2002.

[46] Solerte, S. B.; Ceresini, G.; Ferrari, E.; Fioravanti, M. Hemorheological changes and overproduction of cytokines from immune cells in mild to moderate dementia of the Alzheimer's type: adverse effects on cerebromicrovascular system. *Neurobiol. Aging* **21**:271–281; 2000.

[47] Small, D. H.; Mok, S. S.; Bornstein, J. C. Alzheimer's disease and Aβtoxicity: from top to bottom. *Nat. Rev. Neurosci.* **2**:595–599; 2001.

[48] Borisenko, G. G.; Matsura, T.; Liu, S. X.; Tyurin, V. A.; Jianfei, J.; Serinkan, F. B.; Kagan, V. E. Macrophage recognition of externalized phosphatidylserine and phagocytosis of apoptotic Jurkat cells—existence of a threshold. *Arch. Biochem. Biophys.* **413**:41–52; 2003.

Available online at www.sciencedirect.com
ScienceDirect
Experimental Gerontology 42 (2007) 532–537
Experimental Gerontology
www.elsevier.com/locate/expgero

Induction of matrix metalloproteinases (MMP3, MMP12 and MMP13) expression in the microglia by amyloid-β stimulation via the PI3K/Akt pathway

Sachiko Ito [a], Kenya Kimura [b], Masataka Haneda [a], Yoshiyuki Ishida [c], Makoto Sawada [d], Ken-ichi Isobe [a,*]

[a] *Department of Immunology, Nagoya University Graduate School of Medicine, 65 Turumai-cho, Showa-ku, Nagoya, Aichi, 466-8520, Japan*
[b] *Division of Surgical Oncology, Department of Surgery, Nagoya University Graduate School of Medicine, 65 Turumai-cho, Showa-ku, Nagoya, Aichi, 466-8520, Japan*
[c] *Radioisotope Research Center, Nagoya University, Furo-cho, Chikusa-ku, Nagoya 464-8601, Japan*
[d] *Department of Brain Life Science, Research Institute for Environmental Medicine, Nagoya University, Furo-cho, Chikusa-ku, Nagoya 464-8601, Japan*

Received 21 June 2006; received in revised form 2 November 2006; accepted 21 November 2006
Available online 2 January 2007

Abstract

Alzheimer's disease is characterized by the presence of senile plaques in the brain composed primarily of amyloid-β peptide. Microglia have been reported to surround these Aβ plaques, which have opposite roles, provoking a microglia-mediated inflammatory response that contributes to neuronal cell loss or the removal of Aβ and damaged neurons. We herein analyzed the process of expression of Matrix metalloproteinases induced by Aβ stimulation. We found that Aβ1-42 induces a high level of MMP3, MMP12 and MMP13 in the microglia. The signal transduction pathway for the expression of these MMPs mRNA induced by Aβ1-42 depends on PI3K/Akt.

Keywords: Microglia; Alzheimer's disease; Amyloid β; MMP; Akt

1. Introduction

Alzheimer's disease (AD) is characterized by the presence of senile plaques in the brain composed primarily of amyloid-β peptide (Aβ). Microglia have been reported to surround such Aβ plaques (Haga et al., 1989; Itagaki et al., 1989). Microglia stimulated with Aβ may promote the death of neurons by producing free radicals or cytokines (Meda et al., 1995; Ishii et al., 2000; McDonald et al., 1997). On the contrary, microglia may clear Aβ through phagocytosis (Frautschy et al., 1992; Wyss-Coray et al., 2001; Rogers et al., 2002). In previous work we have shown that Aβ induces proliferation of microglia and produces M-CSF (Ito et al., 2005). These results suggest that innate immune responses may work as pathogenesis of AD.

Microglia belongs to the family of tissue macrophages. Monocytes/macrophages are prominent cells at sites of chronic inflammation and have been shown to produce Matrix metalloproteinases (MMPs), when activated by agents such as LPS, Con A (Wahl and Lampel, 1987; Lu and Wahl, 2005). MMPs have been implicated as being of pathological significance in the extracellular matrix degradation seen in rheumatoid arthritis, osteoarthritis, atherosclerosis, asthma and inflammatory bowel disease (Mahmoodi et al., 2005; Gueders et al., 2005; Naito and Yoshikawa, 2005; Maier et al., 2004). The relationship between MMPs and AD has been suggested. MMPs may prevent disease progression by degradation of Aβ. On the other hand MMPs may engage the disease progression by degrading brain matrix. Here, we investigate the several kinds of MMPs, which are induced by microglia. Further we examined the signaling pathways, which induce the expression of MMPs by Aβ.

* Corresponding author. Tel.: +81 52 744 2135; fax: +81 52 744 2972.
E-mail address: kisobe@med.nagoya-u.ac.jp (K. Isobe).

0531-5565/$ - see front matter © 2006 Elsevier Inc. All rights reserved.
doi:10.1016/j.exger.2006.11.012

2. Materials and methods

2.1. Materials

Synthetic human Aβ1-42 and Aβ25-35 were obtained from Peptide Institute Inc. Aβ25-35 was dissolved in H_2O and Aβ1-42 was dissolved in 0.1% NH_3 according to the manufacturer's instructions. Anti-MMP3 monoclonal antibody was from R&D Systems, Inc. and anti-MMP12 polyclonal antibody was from Santa Cruz Biotechnology, Inc. Anti-phospho-Akt (Serine 473), anti-Akt, antibodies were from Cell Signaling. Wortmannin and PD98059 were from Calbiochem. SB203580 was from Promega. All inhibitors were resolved in DMSO. Mouse recombinant granulocyte-macrophage colony-stimulating factor (mrGM-CSF) was from BD Bioscience Pharmingen.

2.2. Cell culture

The microglial cell line Ra2 was cultured in MGI medium [Eagle's MEM supplemented with 0.2% glucose, 5 μg/ml bovine Insulin (Sigma–Aldrich), 10% fetal bovine serum (FBS, Invitrogen)] and 0.8 ng/ml mrGM-CSF (Ito et al., 2005). Before Aβ-treatment, the Ra2 cells were cultured in an MGI medium without mrGM-CSF for 16 h. Primary microglia and primary astrocytes were prepared using newborn C57BL/6 mice and cultured as described previously (Ito et al., 2005), and cultured in MGI medium containing 0.8 ng/ml mrGM-CSF. Primary neurons were obtained from the cortex of 14-day-old C57BL/6 mouse embryos as described previously (Ito et al., 2005).

2.3. RT-PCR and real-time quantitative RT-PCR

Total RNA was isolated using an RNeasy mini kit (Qiagen) according to the manufacturer's instructions. Two micrograms of total RNA was reverse transcribed to cDNA using SuperScript II Reverse Transcriptase (Invitrogen). Conventional RT-PCR was performed at the condition of 30 cycles for MMPs or 23 cycles for β-actin at 94 °C for 1 min, 60 °C for 1 min and 72 °C for 1 min. Quantitative real-time PCR was performed on Mx3000P (Promega) using the following program: 10 s at 95 °C, followed by 40 cycles of 5 s at 95 °C, 20 s at 60 °C, and a dissociation reaction. The reactions were carried out using 0.5 μl cDNA with SYBR Premix EX Taq (Takara). Specificity of the PCR product was confirmed by examination of dissociation reaction plots. The values were expressed as the relative expression was normalized to β-actin mRNA. For RT-PCR and real-time quantitative PCR, the primers for mouse MMPs and β-actin genes were listed in Table 1.

Table 1
RT-PCR primers

Target (product size)		Sequence (5′-3′)
MMP2 (203 bp)	Sense	CACACCAGGTGAAGGATGTG
	Antisense	AGGGCTGCATTGCAAATATC
MMP3 (173 bp)	Sense	CAGACTTGTCCCGTTTCCAT
	Antisense	GGTGCTGACTGCATCAAAGA
MMP8 (250 bp)	Sense	CCTATTTCTCGTGGCTGCTC
	Antisense	CCCACGGAGTGTGGTAGTAG
MMP9 (228 bp)	Sense	GAAGGCAAACCCTGTGTGTT
	Antisense	AGAGTACTGCTTGCCCAGGA
MMP12 (184 bp)	Sense	CCAAGCATCCCATCTGCTAT
	Antisense	GGTCAAAGACAGCTGCATCA
MMP13 (286 bp)	Sense	TGATGAAACCTGGACAAGCA
	Antisense	TCCTCGGAGACTGGTAATGG
MMP20 (270 bp)	Sense	CTCGTCCTTTGATGCAGTGA
	Antisense	CTTGGGAACCCGAAGTCATA

2.4. Immunoblotting

The cells were lysed in sample buffer (62.5 mM Tris–HCl, pH 6.8, 2% SDS, 10% glycerol, 5% 2-mercaptoethanol, and 5% bromo phenol blue). Next, 50 μg of total protein were resolved by SDS–PAGE and then were transferred to PVDF membranes (Millipore). Cell-conditioned medium was centrifuged at 2000 rpm to remove dead cells and debris, and concentrated 5 times using Biomax-10 (Millipore). Immunoblotting was performed with the appropriate antibody using the enhanced chemiluminescence (ECL) system (Amersham Pharmacia).

2.5. Statistical analysis

The results are expressed as the means ± SD. A statistical analysis was done using the two-tailed student's *t*-test. A *p*-value of <0.05 was considered to be statistically significant.

3. Results

3.1. Induction of MMPs by Aβ in microglia

To identify MMPs induced by Aβ stimulation in microglia, we examined mRNA expression of microglial cell line Ra2 at 16 h after 10 μM Aβ1-42 treatment by Microarray analysis (data not shown). Microarray analysis revealed several MMPs mRNA species responsive to Aβ1-42 over this time frame (Table 2). These MMPs have been shown to be secreted by inflammatory macrophages. To further analyze MMPs induced by Aβ, Ra2 was treated with 10 μM Aβ1-42 for 16 h, and the expression of MMPs was examined by quantitative real-time PCR. Among several MMPs examined, we found the expression of MMP3 (Stromelysin 1), MMP12 (Macrophage elastase) and MMP13 (Collagenase 3) mRNA to be highly increased by Aβ1-42 stimulation (Fig. 1). We examined the time course of the induction of MMPs. As shown in Fig. 2A induction of MMP3 or MMP12 by Aβ1-42 stimulation was appeared at 6 h and lasted for 24 h. Aβ25–35 was also

Table 2
Expression of matrix metalloproteinase (MMP) and tissue inhibitor of metalloproteinase (TIMP)

	Ratio (Aβ/control)	Control	Aβ
MMP1a	Error	−0.036	−0.001
MMP1b	1.06	0.241	0.254
MMP2	−1.04	52.682	50.516
MMP3	64.20	0.043	2.782
MMP7	1.97	0.121	0.238
MMP8	−4.76	7.893	1.657
MMP9	1.05	0.079	0.083
MMP10	12.28	0.015	0.186
MMP11	Error	0.036	−0.069
MMP12	25.96	1.140	29.612
MMP13	7.01	0.284	1.994
MMP14	1.26	0.266	0.337
MMP15	4.82	0.015	0.071
MMP16	Error	0.037	−0.030
MMP17	−1.01	0.754	0.743
MMP19	1.13	0.998	1.132
MMP20	2.23	0.258	0.577
MMP21	1.64	0.539	0.881
MMP23	1.21	0.260	0.315
MMP24	Error	−0.087	0.063
TIMP1	−2.43	0.128	0.053
TIMP2	−1.23	5.314	4.338
TIMP3	1.15	0.135	0.155
TIMP4	−19.23	0.085	0.004

found to induce these MMPs, although the strength of the induction was lower than that of Aβ1-42 stimulation (Fig. 2B). In the primary microglial cells cultured from newborn C57BL/6 mouse brain, MMP3, MMP12 and MMP13 mRNA expression were also induced by Aβ1-42 (Fig. 3). MMP3 was also expressed in primary astrocytes and neurons. The MMP3 mRNA expression in the unstimulated primary astrocytes was higher than that in the primary microglia. Aβ1-42 increased the expression of MMP3 in microglia, astrocytes and neurons. On the other hand MMP12 or MMP13 was up-regulated by Aβ1-42 only in primary microglia. MMP12 or MMP13 was induced by Aβ1-42 in neither astrocytes nor neurons (Fig. 4). We examined the protein expression of MMP3 and MMP12 by immunoblotting. Expression of MMP3 protein in Ra2 cell lysate was not detected by the stimulation of Aβ1-42. However, we could detect the expression of MMP3 in Ra2 cell-conditioned medium. And the expression of MMP3 protein was increased by the stimulation of Aβ1-42 (Fig. 5A). The expression of MMP12 was detected both in cell lysates and cell-conditioned medium. The MMP12 protein expression was increased by the stimulation of Aβ1-42 (Fig. 5B).

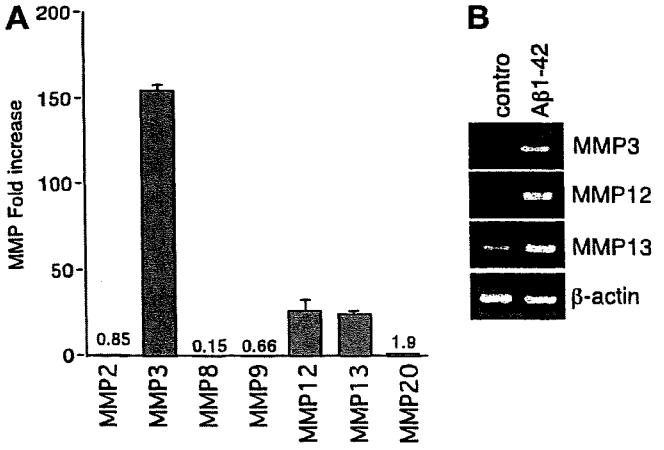

Fig. 1. Ra2 cells were treated with 10 μM Aβ1-42 or 0.1% NH_3 solution as a control for 16 h. (A) Real-time PCR of a series of MMPs mRNA were performed. The result represents the fold increase of Aβ1-42 stimulation to control. Data represent means ± SD of three separate determinations. (B) MMPs and β-actin mRNA were determined by RT-PCR.

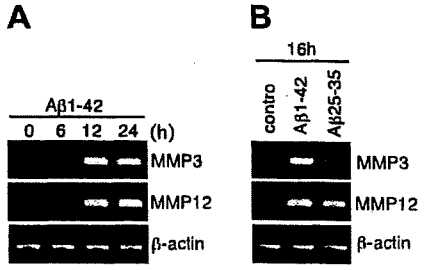

Fig. 2. Aβ stimulates MMP mRNA expressions in Ra2 cells. MMP3, MMP12 and β-actin mRNA expressions were determined by RT-PCR. (A) Time course of MMP expressions in Ra2 cells treated with 10 μM Aβ1-42. (B) Ra2 cells were treated with 10 μM Aβ1-42 or 50 μM 25–35 for 16 h.

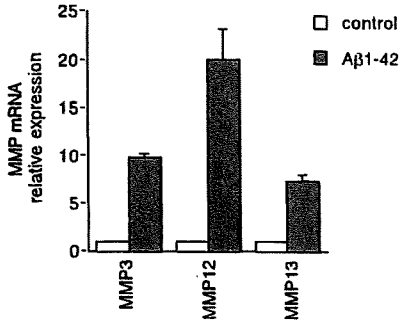

Fig. 3. Induction of MMP3, MMP12 and MMP13 mRNA by Aβ1-42 in primary microglia. Primary microglia was separated from newborn C57BL/6 mouse brain. Cultured cells were treated with 10 μM Aβ1-42 or 0.1% NH_3 solution as a control for 16 h. Extracted RNA was quantified by real-time PCR. The data represent the means ± SD of three separate determinations.

3.2. *Aβ induces the expression of MMP mRNA via the PI3-kinase signal cascade*

Next, we examined the signal cascades for Aβ-induced MMP mRNA expression by using several chemical inhibitors (Fig. 6). Wortmannin, PI3K (phosphatidylinositol 3 kinase) inhibitor, clearly inhibited the induction of MMP mRNA expression by Aβ1-42. However, PD98059, MEK inhibitor and SB203580, p38 inhibitor, did not inhibit the induction of MMP mRNA expression. We analyzed the

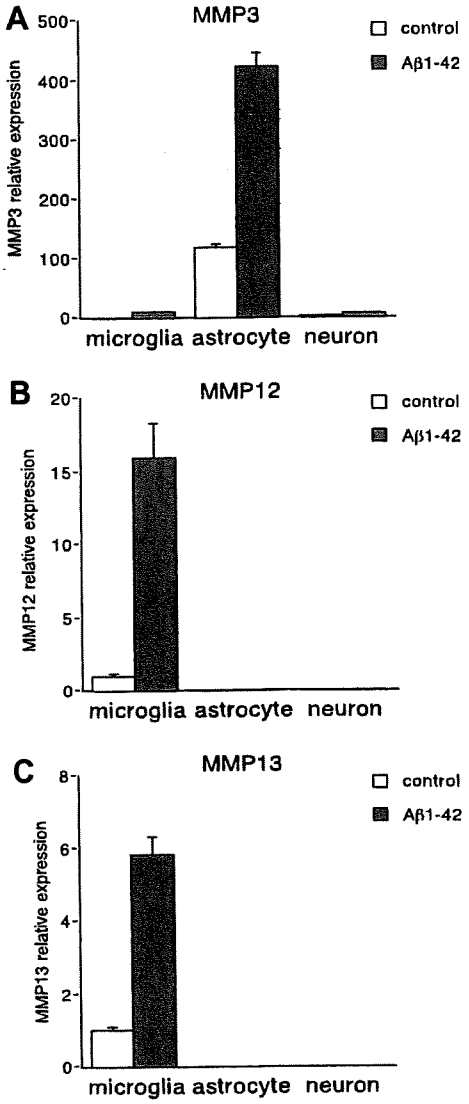

Fig. 4. Induction of MMP3, MMP12 and MMP13 mRNA by Aβ1-42 in primary microglia, primary astrocytes and primary neuron from C57BL/6 mice. Cultured cells were treated with 10 μM Aβ1-42 or 0.1% NH_3 solution as a control for 16 h. Extracted RNA was quantified by real-time PCR. The data represent the means ± SD of three separate determinations.

Akt pathways by immunoblotting. Aβ1-42 induced the phosphorylation of Akt (Fig. 7). The phosphorylation of Akt was sustained up to 2 h (data not shown).

4. Discussion

We have shown in this paper that Aβ1-42 induces the expression of MMP3, MMP12 and MMP13. MMP3 and MMP12 are the family of stromelysin and MMP13 belongs to the family of interstitial collagenases. We found that MMP12 and MMP13 were expressed only in microglia (Fig. 4). They were highly up-regulated by Aβ1-42 stimulation. On the contrary, MMP3 were expressed both in astrocytes and neurons and were weakly expressed in microglia. By the stimulation of Aβ1-42, MMP3 were highly up-reg-

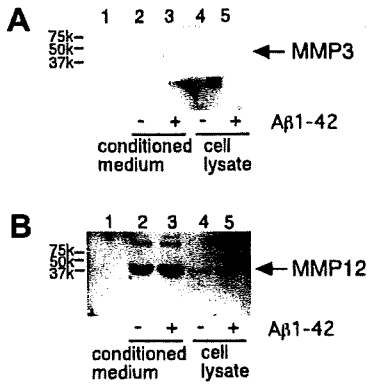

Fig. 5. MMP3 and MMP12 protein expression induced by Aβ1-42. Ra2 cells were treated with 10 μM Aβ1-42 or 0.1% NH_3 solution as a control for 16 h in serum-free medium. Cell-conditioned medium (lanes 2 and 3) and cell lysates (lanes 4 and 5) were immnoblotted using anti-MMP3 antibody (A), and anti-MMP12 antibody (B). Lane 1: serum-free medium as a negative control.

ulated in astrocytes, microglia and neurons. From these results it will be suggested that increase of Aβ1-42 by aging or genetic disorder (Alzheimer's susceptible person) may gradually up-regulate the production of MMP12, and MMP13 by microglia and MMP3 in astrocytes, neurons and also microglia. By using chemical inhibitor, we have herein shown the Aβ-induced activation of MMP3, MMP12 and MMP13 to be correlated with the activation of the PI3K/Akt signaling cascades in the microglia. The expression of MMP12 in SB203580 was higher than the control without or with the stimulation of Aβ1-42 (Fig. 6). SB203580 itself may stimulate the induction of MMP12 mRNA expression. To elucidate more precise signaling pathway by Aβ1-42 stimulation in microglia needs another experiments by using dominant negative or RNAi transfection procedures.

What is the biological function of MMPs in AD? Recent evidence has linked MMPs to various pathological conditions in the central nervous system, including ischemia, multiple sclerosis and AD (Maeda and Sobel, 1996). MMP9 has been shown to be synthesized in neurons of human hippocampus, which is capable of degrading the Aβ (Backstrom et al., 1996). Another aspects of MMPs are related to innate immunity. The lesions that develop, called senile plaques, are extracellular deposits principally composed of insoluble aggregates of Aβ, infiltrated by reactive microglia and astrocytes (Yankner and Mesulam, 1991; Mullan and Crawford, 1993). By using human THP-1 cells, Aβ has been shown to induce MMP9 together with TNF-α (Chong et al., 2001). We have shown that MMP3, MMP12 and MMP13 are up-regulated by Aβ1-42 stimulation. These matrix proteases are a hallmark of inflammation with MMPs considered to be important effectors of inflammatory process and also essential for leukocyte extravasation and migration (Luckow et al., 2004). We have to be in mind that MMPs produced further enhance the inflammatory processes. Recent paper has shown that apoptotic neuronal cells release MMP3, which

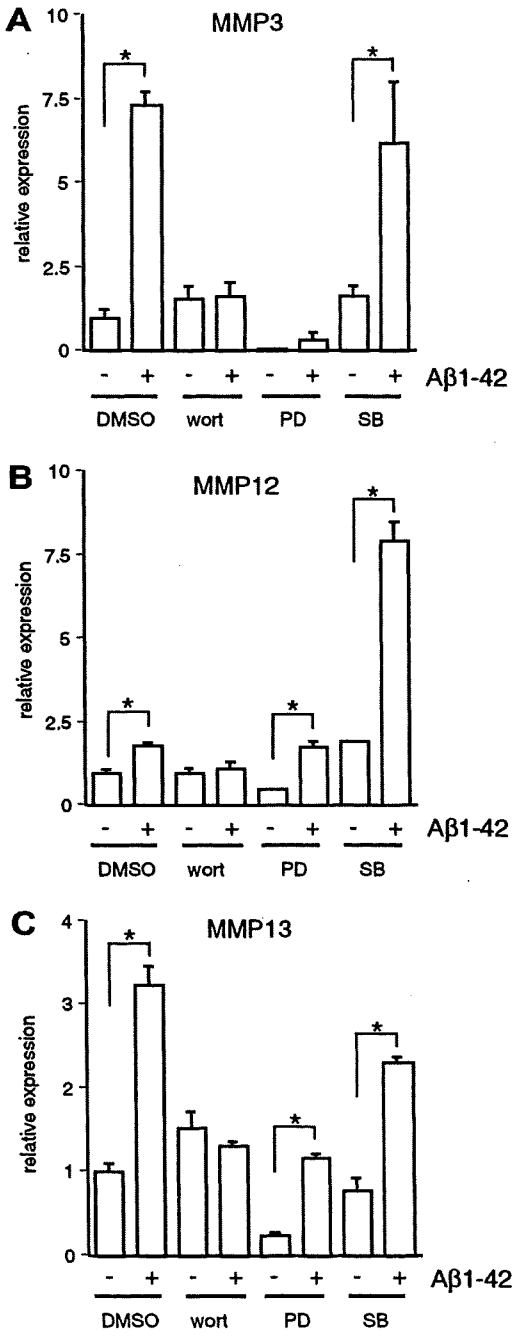

Fig. 6. Signal transduction for (A) MMP3, (B) MMP12 and (C) MMP13 mRNA expression induced by Aβ1-42. Ra2 cells were pre-incubated with 200 nM wortmannin (wort), 10 μM PD98059 (PD) or 10 μM SB203580 (SB) for 30 min before the addition of 10 μM Aβ1-42 or 0.1% NH_3 solution as a control for 6 h. Total RNA was extracted and quantified by real-time PCR. The data represent the means ± SD of three separate determinations (*$p < 0.05$).

induces microglial activation. Activated microglia produces TNFα, IL-6 and IL-1β (Kim et al., 2005). MMP12 has been shown to activate other MMPs such as MMP-2 and MMP-3, by which MMP12 exacerbates the cascade of proteolytic processes (Matsumoto et al., 1998).

It has been reported that MMP1, MMP3 and MMP9 are up-regulated in AD (Asahina et al., 2001; Leake et al., 2000; Lorenzl et al., 2003; Yoshiyama et al., 2000). By these findings genetic association between MMP and AD have been studied. The studies in Finland indicated the interaction between MMP3*5A and APOE 4 alleles increases the risk of AD (Saarela et al., 2004). However, no clear association between MMP3 and MMP9 polymorphisms and AD in Japanese (Shibata et al., 2005). From our results MMP12 and MMP13 may engage in progression of AD. Further works using clinical material are waiting.

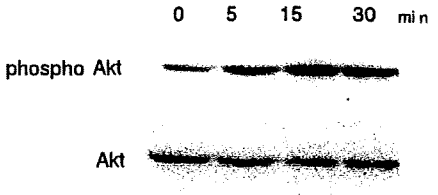

Fig. 7. Aβ1-42 induces the phosphorylation of Akt. Ra2 cells were treated with 10 μM Aβ1-42 for indicated times. Cell lysates were analyzed by immunoblotting using anti-phospho Akt (Ser 473) antibody. The same blot was reprobed with anti-Akt.

Acknowledgements

This study was supported by the Program for the Promotion of Fundamental Studies in Health Sciences of the Organization for Pharmaceutical Safety and Research (of Japan), and in part by grants-in-aid for Scientific Research from the Japanese Ministry of Education, Culture, Sports, Science and Technology.

References

Asahina, M., Yoshiyama, Y., Hattori, T., 2001. Expression of matrix metalloproteinase-9 and urinary-type plasminogen activator in Alzheimer's disease. Brain. Clin. Neuropathol. 20, 60–63.

Backstrom, J.R., Lim, G.P., Cullen, M.J., Tokes, Z.A., 1996. Matrix metalloproteinase-9 (MMP-9) is synthesized in neurons of the human hippocampus and is capable of degrading the amyloid-beta peptide (1–40). J. Neurosci. 16, 7910–7919.

Chong, Y.H., Sung, J.H., Shin, S.A., Chung, J.H., Suh, Y.H., 2001. Effects of the beta-amyloid and carboxyl-terminal fragment of Alzheimer's amyloid precursor protein on the production of the tumor necrosis factor-alpha and matrix metalloproteinase-9 by human monocytic THP-1. J. Biol. Chem. 276, 23511–23517.

Frautschy, S.A., Cole, G.M., Baird, A., 1992. Phagocytosis and deposition of vascular beta-amyloid in rat brains injected with Alzheimer beta-amyloid. Am. J. Pathol. 140, 1389–1399.

Gueders, M.M., Balbin, M., Rocks, N., Foidart, J.M., Gosset, P., Louis, R., Shapiro, S., Lopez-Otin, C., Noel, A., Cataldo, D.D., 2005. Matrix metalloproteinase-8 deficiency promotes granulocytic allergen-induced airway inflammation. J. Immunol. 175, 2589–2597.

Haga, S., Akai, K., Ishii, T., 1989. Demonstration of microglial cells in and around senile (neuritic) plaques in the Alzheimer brain. An immunohistochemical study using a novel monoclonal antibody. Acta. Neuropathol. (Berl.) 77, 569–575.

Ishii, K., Muelhauser, F., Liebl, U., Picard, M., Kuhl, S., Penke, B., Bayer, T., Wiessler, M., Hennerici, M., Beyreuther, K., Hartmann, T., Fassbender, K., 2000. Subacute NO generation induced by Alzheimer's beta-amyloid in the living brain: reversal by inhibition of the inducible NO synthase. FASEB J. 14, 1485–1489.

Itagaki, S., McGeer, P.L., Akiyama, H., Zhu, S., Selkoe, D., 1989. Relationship of microglia and astrocytes to amyloid deposits of Alzheimer disease. J. Neuroimmunol. 24, 173–182.

Ito, S., Sawada, M., Haneda, M., Fujii, S., Oh-Hashi, K., Kiuchi, K., Takahashi, M., Isobe, K., 2005. Amyloid-beta peptides induce cell proliferation and macrophage colony-stimulating factor expression via the PI3-kinase/Akt pathway in cultured Ra2 microglial cells. FEBS Lett. 579, 1995–2000.

Kim, Y.S., Kim, S.S., Cho, J.J., Choi, D.H., Hwang, O., Shin, D.H., Chun, H.S., Beal, M.F., Tong, H., Joh, T.H., 2005. Matrix Metalloproteinase-3: a novel signaling proteinase from apoptotic neuronal cells that activates microglia. J. Neurosci. 25, 3701–3711.

Leake, A., Morris, C.M., Whateley, J., 2000. Brain matrix metalloproteinase 1 levels are elevated in Alzheimer's disease. Neurosci. Lett. 291, 201–203.

Lorenzl, S., Albers, D.S., Relkin, N., Ngyuen, T., Hilgenberg, S.L., Chirichigno, J., Cudkowicz, M.E., Beal, M.F., 2003. Increased plasma levels of matrix metalloproteinase-9 in patients with Alzheimer's disease. Neurochem. Int. 43, 191–196.

Lu, Y., Wahl, L.M., 2005. Oxidative stress augments the production of matrix metalloproteinase-1, cyclooxygenase-2, and prostaglandin E2 through enhancement of NF-kappa B activity in lipopolysaccharide-activated human primary monocytes. J. Immunol. 175, 5423–5429.

Luckow, B., Joergensen, J., Chilla, S., Li, J.P., Henger, A., Kiss, E., Wieczorek, G., Roth, L., Hartmann, N., Hoffmann, R., Kretzler, M., Nelson, P.J., Perez de Lema, G., Maier, H., Wurst, W., Balling, R., Pfeffer, K., Grone, H.J., Schlondorff, D., Zerwes, H.G., 2004. Reduced intragraft mRNA expression of matrix metalloproteinases Mmp3, Mmp12, Mmp13 and Adam8, and diminished transplant arteriosclerosis in Ccr5-deficient mice. Eur. J. Immunol. 34, 2568–2578.

Maeda, A., Sobel, R.A., 1996. Matrix metalloproteinases in the normal human central nervous system, microglial nodules, and multiple sclerosis lesions. J. Neuropathol. Exp. neurol. 55, 300–309.

Maier, H., Wurst, W., Balling, R., Pfeffer, K., Grone, H.J., Schlondorff, D., Zerwes, H.G., 2004. Reduced intragraft mRNA expression of matrix metalloproteinases Mmp3, Mmp12, Mmp13 and Adam8, and diminished transplant arteriosclerosis in Ccr5-deficient mice. Eur. J. Immunol. 34, 2568–2578.

Mahmoodi, M., Sahebjam, S., Smookler, D., Khokha, R., Mort, J.S., 2005. Lack of tissue inhibitor of metalloproteinases-3 results in an enhanced inflammatory response in antigen-induced arthritis. Am. J. Pathol. 166, 1733–1740.

Matsumoto, S., Kobayashi, T., Katoh, M., Saito, S., Ikeda, Y., Kobori, M., Masuho, Y., Watanabe, T., 1998. Expression and localization of matrix metalloproteinase-12 in the aorta of cholesterol-fed rabbits: relationship to lesion development. Am. J. Pathol. 153, 109–119.

McDonald, D.R., Brunden, K.R., Landreth, G.E., 1997. Amyloid fibrils activate tyrosine kinase-dependent signaling and superoxide production in microglia. J. Neurosci. 17, 2284–2294.

Meda, L., Cassatella, M.A., Szendrei, G.I., Otvos Jr., L., Baron, P., Villalba, M., Ferrari, D., Rossi, F., 1995. Activation of microglial cells by beta-amyloid protein and interferon-gamma. Nature 374, 647–650.

Mullan, M., Crawford, F., 1993. Genetic and molecular advances in Alzheimer's disease. Trends Neurosci. 16, 398–403.

Naito, Y., Yoshikawa, T., 2005. Role of matrix metalloproteinases in inflammatory bowel disease. Mol. Aspects. Med. 26, 379–390.

Rogers, J., Strohmeyer, R., Kovelowski, C.J., Li, R., 2002. Microglia and inflammatory mechanisms in the clearance of amyloid beta peptide. Glia 40, 260–269.

Saarela, M.S., Lehtimaki, T., Rinne, J.O., Hervonen, A., Jylha, M., Roytta, M., Ahonen, J.P., Mattila, K.M., 2004. Interaction between matrix metalloproteinase 3 and the epsilon4 allele of apolipoprotein E increases the risk of Alzheimer's disease in Finns. Neurosci. Lett. 367, 336–339.

Shibata, N., Ohnuma, T., Higashi, S., Usui, C., Ohkubo, T., Kitajima, A., Ueki, A., Nagao, M., Arai, H., 2005. Genetic association between matrix metalloproteinase MMP9 and MMP3 polymorphisms and Japanese sporadic Alzheimer's disease. Neurobiol. Aging 26, 1011–1014.

Wahl, L.M., Lampel, L.L., 1987. Regulation of human peripheral blood monocyte collagenase by prostaglandins and anti-inflammatory drugs. Cell. Immunol. 105, 411–422.

Wyss-Coray, T., Lin, C., Yan, F., Yu, G.Q., Rohde, M., McConlogue, L., Masliah, E., Mucke, L., 2001. TGF-beta1 promotes microglial amyloid-beta clearance and reduces plaque burden in transgenic mice. Nat. Med. 7, 612–618.

Ya nkner, B.A., Mesulam, M.M., 1991. Seminars in medicine of the Beth Israel Hospital, Boston. beta-Amyloid and the pathogenesis of Alzheimer's disease. N. Engl. J. Med. 325, 1849–1857.

Yoshiyama, Y., Asahina, M., Hattori, T., 2000. Selective distribution of matrix metalloproteinase-3 (MMP-3) in Alzheimer's disease brain. Acta. Neuropathol. (Berl.) 99, 91–95.

The Effects of General Anesthetics on $P2X_7$ and P2Y Receptors in a Rat Microglial Cell Line

Mika Nakanishi, MD*

Takashi Mori, MD, PhD*

Kiyonobu Nishikawa, MD, PhD*

Makoto Sawada, PhD†

Miyuki Kuno, MD, PhD‡

Akira Asada, MD, PhD*

BACKGROUND: Microglial cells play important roles in coordinating the inflammatory brain responses to hypoxia and trauma. Ionotropic P2X receptors and metabotropic P2Y receptors (P2YRs) expressed in microglia can be activated by extracellular adenosine triphosphate (ATP) derived from damaged cells or astrocytes, and participate in the signaling pathways evoked in brain insult. Although several inhaled and IV anesthetics produce neuroprotective effects through neuronal mechanisms, little is known about how general anesthetics modulate microglial responses in the pathological state. We examined the effects of various general anesthetics on purinergic responses in a rat microglial cell line.

METHODS: Currents were consistently activated by applications of ATP via a U-tube system under the whole-cell configuration. ATP-induced nondesensitizing currents observed after several applications of ATP exhibited characteristics of $P2X_7$ receptors. The P2YRs-mediated mobilization of intracellular Ca^{2+} was measured using a Ca^{2+}-sensitive fluorescent dye (fura-2).

RESULTS: Inhaled anesthetics (sevoflurane, isoflurane, and halothane) at doses three times as high as minimum alveolar concentrations had no effect on the $P2X_7$Rs-mediated currents. IV anesthetics (ketamine, propofol, and thiopental) enhanced the $P2X_7$Rs-mediated currents reversibly. The potencies for activation of $P2X_7$Rs were not correlated with the octanol/buffer partition coefficients. Thiopental, at low concentrations, slightly inhibited the $P2X_7$Rs-mediated currents, suggesting its dual actions on $P2X_7$Rs. The P2YRs-mediated mobilization of intracellular Ca^{2+} was not affected by any of the general anesthetics tested.

CONCLUSIONS: Our results suggest that IV anesthetics, particularly thiopental and propofol, may modulate microglial functions through $P2X_7$Rs in pathological conditions.

(Anesth Analg 2007;104:1136-44)

Microglia, the principle immune cells of the central nervous system (CNS), play crucial roles in regulating inflammatory responses to ischemic brain damage, traumatic injury, and neurodegenerative diseases (1,2). Microglia activated during brain insult performs phagocytosis, migration, proliferation, and release of a number of biologically active substances (1). Microglial functions are basically neuroprotective (host defense, tissue repair), but over-stimulation of their immune reactions may result in acceleration of neuronal damage after brain insult (3,4). Therefore, the regulation of microglial functions are thought to provide new modalities in therapeutic intervention against CNS disorders where inflammatory activation of microglia is involved (2,5).

Extracellular adenosine triphosphate (ATP) derived from injured cells or astrocytes is one of the most important key messengers for mediating pathological conditions of the CNS. Massive amounts of ATP are released from damaged tissue after ischemia and trauma, resulting in sustained elevation of ATP levels in the areas surrounding the injured zone (6–8). Microglia express various types of ionotropic (P2X: $P2X_4$, $P2X_7$) and metabotropic ATP receptors (P2Y: $P2Y_2$, $P2Y_4$, $P2Y_{12}$) (5,9). The former receptors are nonselective cation channels, and are responsible for depolarization and Ca^{2+} influx (10), whereas the latter receptors, coupled with G-protein, activate phospholipase C, inositol-phosphate formation and cause the release of Ca^{2+} from intracellular stores (11). Activation of these P2 receptors leads to production of

From the *Department of Anesthesiology and Intensive Care Medicine, Graduate School of Medicine, Osaka City University, Osaka, Japan; †Department of Brain Science, Research Institute of Environmental Medicine, Nagoya University, Nagoya, Aichi, Japan; and ‡Department of Physiology, Graduate School of Medicine, Osaka City University, Osaka, Japan.

Accepted for publication January 25, 2007.

Supported, in part, by the Japanese Ministry of Education, Culture, Sports, Science and Technology, Tokyo, Japan grant 15790827.

Address correspondence to Mika Nakanishi, MD, Department of Anesthesiology and Intensive Care Medicine, Graduate School of Medicine, Osaka City University, 1-5-7 Asahi-machi, Abeno-ku, Osaka 545-8586, Japan. Address e-mail to m1383144@med.osaka-cu.ac.jp.

Reprint requests to Takashi Mori, MD, Department of Anesthesiology and Intensive Care Medicine, Graduate School of Medicine, Osaka City University, 1-5-7 Asahi-machi, Abeno-ku, Osaka 545-8586, Japan. Address e-mail to m1377033@med.osaka-cu.ac.jp.

DOI: 10.1213/01.ane.0000260615.12553.4e

diverse microglial responses. $P2X_4$ receptors ($P2X_4Rs$) in spinal microglia have been shown to be involved in generating refractory pain and are recognized as a new target for the treatment of neuropathic pain (12). $P2X_7$ receptors ($P2X_7Rs$) are responsible for the release of interleukin-1β, plasminogen, tumor necrosis factor-α, nitric oxide, and superoxide and, furthermore, apoptotic cell death (13–18). P2Y receptors (P2YRs) are related to microglial activation and motility (5), for instance, mitotic activity through activation of $P2Y_2$ and $P2Y_4$ receptors, and chemotaxis through $P2Y_{12}$ receptors (9,19,20). Several recent studies have suggested that $P2X_7Rs$ and P2YRs participate in neuronal damage caused by ischemic and traumatic brain injury (21–24).

Much attention has been given to the neuroprotective effect of general anesthetics in ischemic brain damage (25). Several inhaled and IV anesthetics alleviate neuronal injury induced by focal cerebral ischemia or forebrain ischemia and reduce glutamate neurotoxicity. These neuroprotective effects have mostly been explained by actions of the anesthetics on neurons. However, the effect of general anesthetics on microglia-associated inflammatory processes remains to be defined. In the present study, we investigated the effects of various inhaled and IV anesthetics on $P2X_7Rs$ and P2YRs in a rat microglial cell line.

METHODS

Cell Preparations

A rat microglial cell line (GMI-R1) (26,27) was used in the present study. GMI-R1, an immortalized microglial clone, was established from a rat primary microglial culture similarly as described for the mouse Ra2 cell line (26,27). The characteristics of GMI-R1 cells were considered almost similar to those of microglia in primary culture (28,29). GMI-R1 cells were cultured in Eagle's MEM (Nissui Pharmac., Tokyo, Japan) supplemented with 10% fetal calf serum (Equitech-Bio, Ingram, TX), 0.5–2 ng/mL recombinant mouse GM-CSF (PeproTech, London, UK) containing 100 U/mL penicillin, 0.1 mg/mL streptomycin, and 0.25 ng/mL amphotericin B at 37°C in a humidified atmosphere of 95% air and 5% CO_2. The culture medium was changed every 3–4 d. For patch clamp experiments, cells were plated at a density of $1.0–2.0 \times 10^5$ cells/mL on coverslips and were cultured for 1–3 d. The procedure for culture of GMI-R1 rat microglial cell line was described elsewhere (26,27).

Electrophysiology

A whole-cell patch clamp technique was used to record ionic currents induced by ATP application through a U-tube system. Recording pipettes were pulled in two stages on a vertical pipette puller (Narishige PP-830, Tokyo, Japan). The pipette solution contained 130 mM KCl, 1 mM $CaCl_2$, 2 mM $MgCl_2$, 10 mM EGTA, and 10 mM HEPES-KOH (290 mOs). The external solution contained 140 mM NaCl, 5 mM KCl, 2.5 mM $CaCl_2$, 1 mM $MgCl_2$, 10 mM D-glucose, and 10 mM HEPES-NaOH (290 mOs). The pH of the internal and external solutions was adjusted to 7.3 with KOH and NaOH, respectively. The pipette resistance was about 5 MΩ. The series resistance and the electrode capacitance were compensated and checked before and after pharmacological manipulations to ascertain the constant recording condition. The currents were recorded with a patch clamp amplifier (AXOPATCH 200A, Axon Instruments, Union City, CA) while a membrane potential was held at −60 mV. Current signals were filtered at 5 kHz, digitized at 1–10 kHz via AD converter (Digidata 1200, Axon Instruments), and analyzed using pCLAMP 9 software package (Axon Instruments). Glass coverslips bearing microglial cells were placed in a recording chamber (approximately 2 mL volume) where the external solution was perfused at a rate of 1–2 mL/min. ATP and general anesthetics were applied by a gravity-fed U-tube system placed within 30–50 μm of the target cell. The application times were controlled by computer-driven solenoid valves (General Valve, Fairfield, NJ). This device permitted us to exchange the solution around the cell within 50 ms. (30) To determine the effects of the general anesthetics on ATP-induced currents, all anesthetics were simultaneously applied with ATP from the U-tube onto the cells. All experiments were performed at room temperature (20°C–25°C).

Measurement of Intracellular Ca^{2+} Concentration

The intracellular Ca^{2+} concentration of single cells was determined with a digital fluorescence microscopy (Attofluor, Atto Bioscience, Rockville, MD) using a Ca^{2+}-sensitive fluorescent dye, fura-2. Cells were loaded with the acetoxymethyl ester form of fura-2 (fura-2 AM, Dojindo, Kumamoto, Japan) (5 μM) for 15 min at 37°C in the following external solution: 140 mM NaCl, 5 mM KCl, 1 mM $CaCl_2$, 1 mM $MgCl_2$, 10 mM D-glucose, 10 mM HEPES-NaOH, pH 7.4. After washing the dye, the ratios of fluorescent images (the emission wavelength ≥520 nm) excited at two wavelengths (340 and 380 nm) were measured every 5 s with 30–100 ms exposures. Data (80–120 pixels for each cell) for each illumination were averaged and plotted against time.

During the experimental session, the solution in the glass-bottom dish (2 mL volume) was continuously perfused by external solutions at a rate of 5 mL/min. The extracellular Ca^{2+} was reduced to approximately 100 nM by the mixture of Ca^{2+} and EGTA a few minutes before stimulation. The low Ca^{2+} solution had the following composition: 140 mM NaCl, 5 mM KCl, 1 mM $CaCl_2$, 1 mM $MgCl_2$, 1.5 mM EGTA, 10 mM D-glucose, 10 mM HEPES-NaOH, pH 7.4. ATP and/or anesthetics were dissolved in the low Ca^{2+} solution. At the end of each experiment, the Ca^{2+} responses were normalized by the maximal fluorescence ratio

obtained by adding 10 μM ionomycin in the presence of 1 mM Ca^{2+}. Ten to 30 cells were analyzed at the same time. Recordings were made at room temperature (20°C–25°C).

Materials and Solutions

ATP (Sigma-Aldrich, St. Louis, MO) was dissolved in the external solution at appropriate concentrations immediately before the experiments. The pH of ATP solution was adjusted to 7.4 by NaOH. Oxidized ATP (oATP) and Bz-ATP (all from Sigma-Aldrich) were dissolved in the external solution. Fura-2 stock solution was prepared by adding 50 μg of 75% dimethyl sulfoxide (DMSO) + 25% pluronic acid.

Saturated solutions of inhaled anesthetics (sevoflurane, isoflurane, halothane) were prepared by stirring each inhaled anesthetic in the external solution over 8 h in a sealed glass container with very little air space. In each experiment, inhaled anesthetics were prepared immediately before use by diluting the saturated solutions and were kept in air-free, closed glass bottles to prevent evaporation. The saturated concentrations of inhaled anesthetics were estimated to be 11.8 mM for sevoflurane, 15.3 mM for isoflurane, and 18 mM for halothane. To prevent evaporation of inhaled anesthetics, a gas-tight glass syringe and Teflon tube were used in the perfusion system (30,31).

Ketamine (Sigma-Aldrich) and thiopental (Sigma-Aldrich) were dissolved in the external solution and the pH of test solutions was adjusted to 7.3. Concentrated stock solutions of propofol (Sigma-Aldrich) and ionomycin (Sigma-Aldrich) were dissolved in DMSO. These stock solutions were diluted to appropriate concentrations with the external solution immediately before each application (<0.1% v/v DMSO). DMSO (<0.1%, v/v) had no effects on $P2X_7Rs$-mediated currents and P2YRs-mediated Ca^{2+} mobilization.

Statistics

Data were expressed as the mean ± SEM. For evaluation of general anesthetic action on $P2X_7Rs$ and P2YRs, analysis of variance or *t*-test was performed to assess the significance of differences. $P < 0.05$ was considered statistically significant.

RESULTS

ATP-Induced Currents in Rat Microglia

Most GMI-R1 cells were small round cells in medium supplemented with GM-CSF. These cells are considered to be in an activated state rather than a resting state, although they are somewhat different from microglia activated by a variety of substances such as lipopolysaccharide (28). GMI-R1 cells also express abundant voltage-gated proton channels, consistent with a characteristic of activated microglia in primary culture (29,32).

ATP induced an inward current at −60 mV in most GMI-R1 cells. Figure 1A shows representative currents induced by the first application of ATP from a U-tube

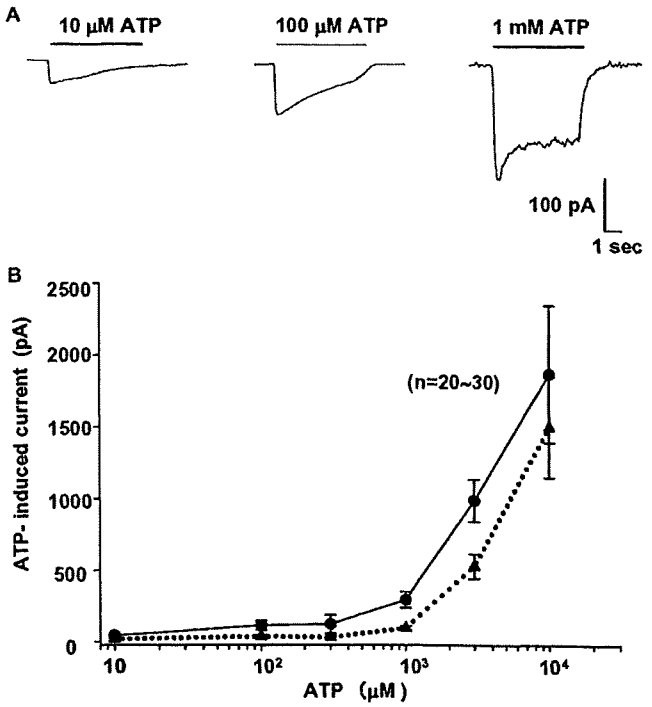

Figure 1. (A) ATP-induced currents in rat microglia. Current traces induced by the first application of ATP through a U-tube for 5 s are shown. The holding potential was −60 mV. ATP-induced currents seemed to consist of desensitizing and nondesensitizing components. (B) ATP concentration–response curves for the peak (circles) and the steady-state currents (triangles). The peak amplitudes were obtained from currents induced by the first applications of ATP in each cell. The amplitudes of nondesensitizing component (steady-state currents) were estimated from fitting the decay phase of the currents with single exponential function. Data are given as mean ± SEM.

onto each cell for 5 s. The ATP-induced current was increased in a concentration-dependent manner. The lowest effective concentration to elicit visible currents in almost half of the cells was 1 μM. ATP higher than 10 mM was not tested since it caused severe cell damage. ATP-induced currents seemed to consist of desensitizing and nondesensitizing components. Dose–responses of the peak amplitudes (circles) and nondesensitizing amplitudes (triangles) are plotted in Figure 1B. The amplitudes of nondesensitizing components were extrapolated by fitting the decay phase of the currents with single exponential function. We could not calculate the EC_{50} for each of the two components because of the lack of the maximum response. The currents induced by 100 μM and 1 mM ATP could well represent those two types of P2X receptors, one exhibiting desensitizing currents and the other, nondesensitizing currents.

The ATP-induced desensitizing currents were further characterized. At a concentration of 100 μM, currents desensitized rapidly (Fig. 1A). The currents were observed in cells pretreated with the $P2X_7Rs$ antagonist, oATP (2 mM), for 1–2 h (10). Thus the desensitized currents seem to be mediated by $P2X_4Rs$.

At 1 mM ATP, the currents comprised desensitizing and nondesensitizing currents as well (Fig. 1A, right).

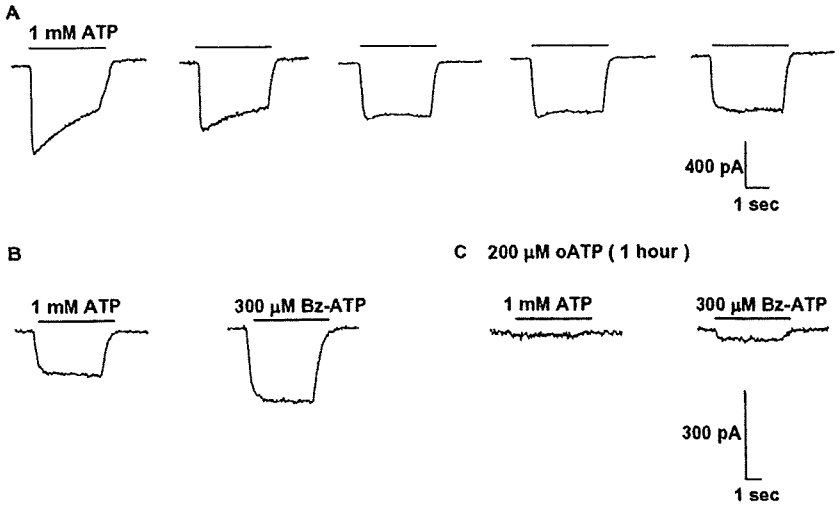

Figure 2. (A) Isolation of $P2X_7$ receptor-mediated currents. The currents (−60 mV) induced by the first application of ATP (1 mM) comprise two types of currents; a desensitizing component and a nondesensitizing component. After repetitive applications of 1-mM ATP for three to six times, the desensitizing component disappeared and only the nondesensitizing component remained in all cells tested. (B) The nondesensitizing currents were also activated with Bz-ATP (300 μM), a specific agonist of $P2X_7Rs$. (C) The currents were almost completely blocked after 1 h treatment with oATP (200 μM). Current traces shown in B and C were recorded in the same cell.

After repetitive (3–6 times) applications of 1 mM ATP, the desensitizing component disappeared and only the nondesensitizing component remained in all cells tested (Fig. 2A). Applications of ATP at an interval of 2 min ensured a stable response of the nondesensitizing currents. The nondesensitizing currents were also activated by Bz-ATP, a specific agonist of $P2X_7Rs$ (Fig. 2B) and blocked by oATP, an antagonist of P2XRs (Fig. 2C) ($n = 5$), indicating that they were mediated mostly via $P2X_7Rs$.

The electrophysiological features of P2XRs in the microglial cell line were similar to those reported in rat microglia in primary culture (10). In later experiments, we focused on investigating the effects of general anesthetics on $P2X_7R$-mediated currents, because $P2X_7Rs$ are thought to be important in the process of microglial inflammatory responses during prolonged exposure to ATP in pathological conditions such as ischemic brain damage, traumatic injury, and neurodegenerative diseases (5,17,21,24).

Effects of General Anesthetics on $P2X_7Rs$

The effects of general anesthetics on ATP-induced currents via $P2X_7Rs$ were examined after $P2X_4Rs$ were desensitized. First we tested inhaled anesthetics (sevoflurane, isoflurane). These anesthetics did not generate currents when applied alone ($n = 5$) (Fig. 3A). The $P2X_7Rs$-mediated currents were unchanged by coapplication of ATP and anesthetics at doses three times as high as the minimum alveolar concentrations (990 μM for sevoflurane, 840 μM for isoflurane, and 690 μM for halothane) (Fig. 3B). $P2X_7Rs$-mediated current was not affected even when isoflurane was preperfused in the bath for 2 min (Fig. 3C, right). As with coapplication, preperfusion of isoflurane (840 μM) had no effect on $P2X_7Rs$ (97% ± 12% for coapplication and 94% ± 7% for preperfusion, $n = 3$). Figure 3D summarizes the effects of anesthetics on ATP-induced currents. Even 10 minimum alveolar concentrations of sevoflurane (3300 μM) was ineffective.

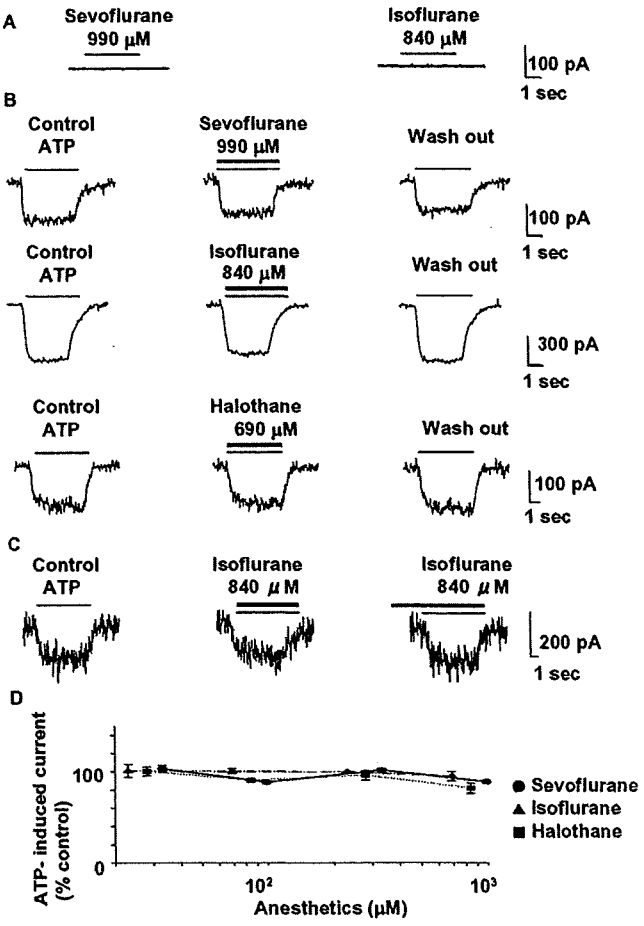

Figure 3. Effects of inhaled anesthetics on $P2X_7Rs$-mediated currents. (A) Sevoflurane and isoflurane themselves induced no currents ($n = 5$). (B) Representative traces of the effects of inhaled anesthetics on $P2X_7Rs$-mediated currents. The currents were induced by 1 mM ATP. Inhaled anesthetics were coapplied with ATP via a U-tube. (C) $P2X_7Rs$-mediated current was not affected even when isoflurane (840 μM) was preperfused in the bath for 2 min (right). (D) Sevoflurane, isoflurane, and halothane had no effect on $P2X_7Rs$-mediated currents at doses up to three times as high as the minimum alveolar concentration (MAC) in all cells tested ($n = 14$, 5, and 5, respectively). The holding potential was −60 mV. Data are given as mean ± SEM.

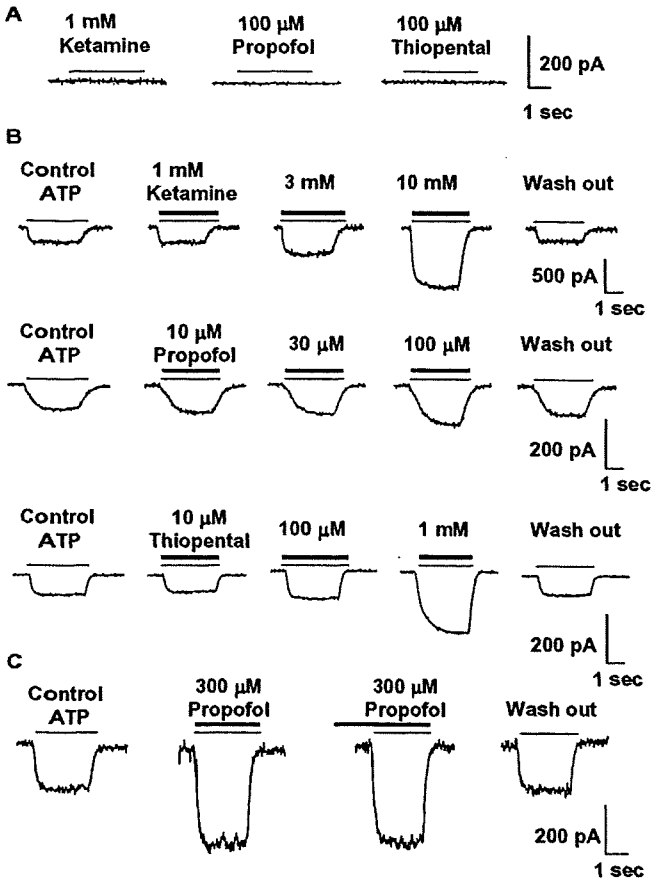

Figure 4. Effects of IV anesthetics on $P2X_7Rs$-mediated currents. (A) Ketamine, propofol, and thiopental themselves had no effect on the currents (−60 mV). (B) Ketamine, propofol, and thiopental increased the $P2X_7Rs$-mediated currents in a dose-dependent manner. ATP was 1 mM. These effects were reversible after washout of the anesthetics. (C) Traces show preperfusion of propofol produced no additional effect on $P2X_7Rs$-mediated currents as compared with coapplication.

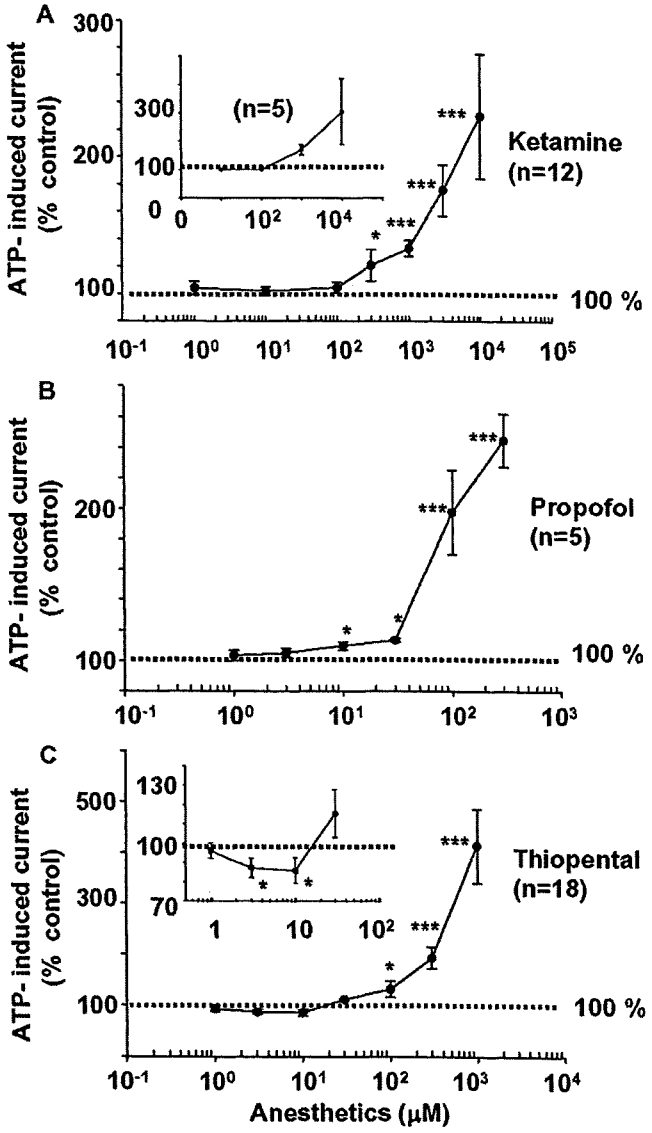

Figure 5. Dose–response relationships of IV anesthetics for $P2X_7Rs$-mediated currents induced by 1 mM ATP. Ordinate represents the current amplitude as percentages of the control. Ketamine (A), propofol (B), and thiopental (C) enhanced the $P2X_7Rs$-mediated currents at concentrations higher than 300, 10, and 100 μM, respectively. Ketamine-induced enhancement at 300 μM ATP was not significantly different from that at 1 mM ATP (A, inset). Thiopental reduced the currents at lower concentrations (C, inset). Data are means ± SEM. Asterisks indicate significant difference from the control ($^*P < 0.05$, $^{***}P < 0.005$) (paired *t*-test).

Next, the effects of IV anesthetics such as ketamine, propofol, and thiopental on $P2X_7Rs$ were examined. Although these anesthetics alone induced no currents ($n = 5$) (Fig. 4A), they enhanced the ATP-induced currents in a dose-dependent manner (Figs. 4B and 5). The enhancement of $P2X_7Rs$ was reversible after washing with anesthetic-free solutions (Fig. 4B, right column). Figure 4C shows that preperfusion of propofol (300 μM) produced no additional effect on $P2X_7Rs$-mediated currents as compared with coapplication. There were no differences in the effect of ketamine, propofol, and thiopental on $P2X_7Rs$-mediated currents between the two application methods, preperfusion and coapplication. The enhancing effects of preperfusion and coapplication as assessed by the percentage of control were 155% ± 16% and 162% ± 22% for 1 mM ketamine, 402% ± 170% and 397% ± 160% for 300 μM propofol, and 182% ± 7% and 174% ± 13% for 300 μM thiopental ($n = 3$, each drug). Significant enhancement was observed at 300 μM for ketamine (Fig. 5, top), 10 μM for propofol (middle), and 100 μM thiopental (bottom) (paired *t*-test). From the dose–response relationships, the effective concentrations to increase $P2X_7Rs$-mediated currents to 125% and 150% of the control (EC_{125} and EC_{150}), respectively, were 570 and 1790 μM for ketamine, 40 and 60 μM for propofol, and 76 and 160 μM for thiopental. The potencies for activation of $P2X_7Rs$ were correlated neither with potencies in inducing general anesthesia nor with the octanol/buffer partition coefficients (33,34). The enhancing effects of ketamine and propofol were compared between two concentrations of ATP (300 μM and 1 mM). Ketamine-induced enhancement at 300 μM ATP (Fig. 5A, inset) was not significantly different from that at 1 mM ATP. The enhancement by propofol